

表面等离子体共振和局域表面等离子体共振技术在病毒检测领域的研究进展

徐厚祥, 徐彬^{***}, 熊吉川^{**}, 刘学峰^{*}

南京理工大学电子工程与光电技术学院, 江苏 南京 210094

摘要 高传染性病毒对生命安全和运行有重大的威胁, 快速灵敏的病毒检测是防止病毒爆发的首要手段。基于表面等离子体共振 (SPR) 和局域表面等离子体共振 (LSPR) 技术的生物传感器具有快速、高灵敏等特点, 在临床病毒检测上有巨大的应用潜力。从抗体、抗原、核酸和病毒颗粒这四类传感器捕获物入手, 基于四种病毒检测方法, 综述了 SPR 和 LSPR 传感器的最新研究成果, 对其中应用的传感策略和结合的优化技术进行了分类介绍, 并通过对比传感器的检测限, 阐述了检测限差距产生的原因。最后, 汇总了近十五年来 SPR 和 LSPR 病毒传感器的各项参数, 对 SPR 和 LSPR 传感器在病毒检测领域中的进展进行了总结和展望。

关键词 生物技术; 表面等离子体; 表面等离子体共振; 局域表面等离子体共振; 病毒检测; 生物传感器

中图分类号 O535

文献标志码 A

DOI: 10.3788/CJL202249.1507401

1 引言

2009 年, 甲型 H1N1 流行性感在墨西哥和美国爆发, 波及 214 个国家, 导致至少 1.4 万人死亡^[1]。2020 年爆发的新型冠状病毒肺炎疫情由于难以快速实时防疫检测等原因, 历经两年仍在全球肆虐^[2]。其他如登革病毒 (DENV)、人类免疫缺陷病毒 (HIV) 等病毒的传播也一直影响着人们的身体健康, 而病毒检测就是遏制病毒传播的关键。

病毒检测的方法主要分为抗体检测、病毒抗原检测、病毒核酸检测和病毒颗粒检测^[3-7]。基于病毒抗原/抗体检测的酶联免疫吸附试验 (ELISA) 能够根据检测到的抗原/抗体水平判别病毒感染情况^[8-9]。基于核酸检测的聚合酶链反应 (PCR) 作为应用最成功的技术之一, 能够以相对较低的样品成本, 高通量检测病毒的核糖核酸 (RNA)/脱氧核糖核酸 (DNA)^[10-11]。ELISA 和 PCR 虽然可以检测病毒, 但是需要将样品收集到实验室, 由专业人员进行病毒分离和测定, 才能得出准确结果, 极大地减缓了病毒检测速度^[3]。为了及时发现并阻断病毒传播, 人们对病毒检测方法提出了快速、高灵敏、特异性的要求, 而基于表面等离子体共振 (SPR) 和局域表面等离子体共振 (LSPR) 技术的部分生物传感器展示出的检测限已经不亚于 ELISA 和 PCR 检测方法^[12-13], SPR 和 LSPR 技术在病毒检测领域中表现出了巨大的应用潜力。

表面等离子体共振是入射光波在金属膜-电介质界面上引起的自由电子的集体振荡运动, 这种共振在两种介质中以指数衰减形式传播, 当金属表面的识别元件捕获到病毒时, 金属表面折射率发生改变, 而 SPR 共振角与金属表面折射率相关, SPR 共振角的改变能够表征 SPR 传感器金属层表面样品状态的改变, 进而实现病毒检测^[14-15]。局域表面等离子体共振是一种将共振电磁场控制在金属微纳结构内的 SPR 现象, 该微纳结构的尺寸比入射光波波长短, 微纳结构的吸收和散射光谱对其形状、尺寸、介电性能以及周围介质介电性能的改变十分敏感^[16-19], 在微纳结构的表面修饰物捕获到病毒分析物后, LSPR 传感器产生吸收峰偏移, 从而实现病毒检测^[20]。

区别于以往相关综述^[21-24], 本文针对四种病毒通用的检测方法, 从 SPR 和 LSPR 传感器捕获到的四类目标分析物出发, 分析梳理了最新的相关研究进展, 如图 1 所示。

2 SPR/LSPR 传感器检测抗体

抗体检测传感器通常是基于抗原 (Ag) 和抗体 (Ab) 的特异性结合原理, 通过在 SPR 和 LSPR 传感器表面修饰特定抗原, 对血清或其他生物体液样本内的对应抗体进行检测^[25]。抗体检测与抗原检测相比, 具有更长的检测窗口, 与病毒核酸检测相比, 抗体样本在采集、运输和检测过程中有较好的稳定性。抗体检

收稿日期: 2021-12-07; 修回日期: 2022-01-22; 录用日期: 2022-02-17

基金项目: 国家自然科学基金 (61827814, 62105155)、北京市自然科学基金 (Z190018)

通信作者: *liuxf_1956@sina.com; **jichuan.xiong@njust.edu.cn; ***xubinhit13@163.com

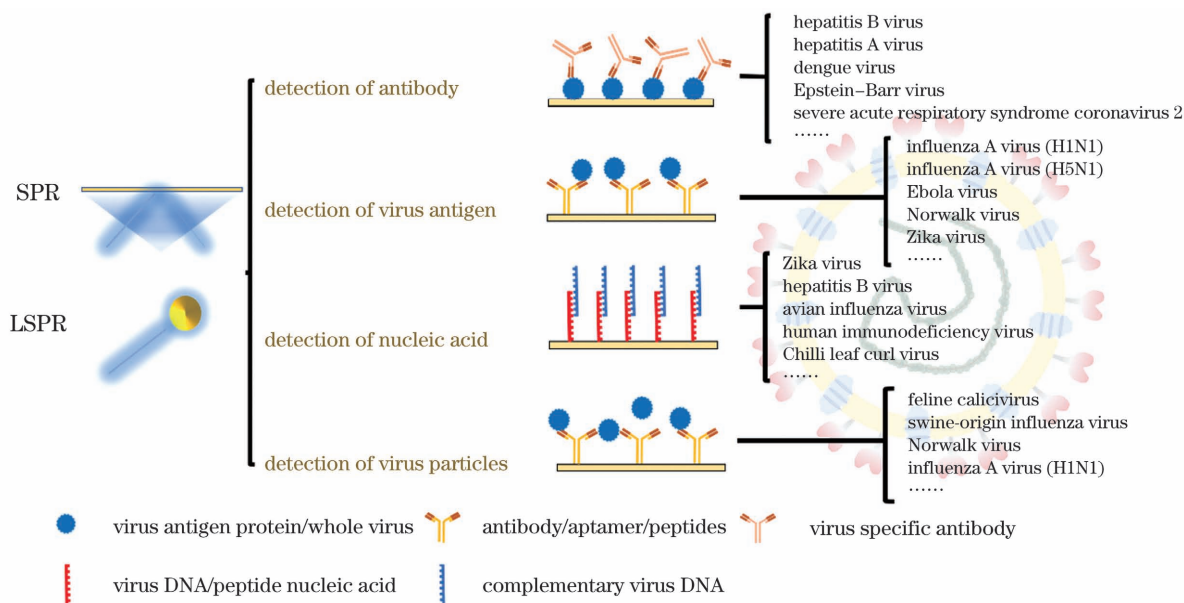


图 1 基于 SPR 或 LSPR 技术的病毒检测方法

Fig. 1 Methods for virus detection based on SPR or LSPR technique

测在既往感染史检测、疫苗评估等方面有重要应用^[26-28],尤其是针对免疫球蛋白 M(IgM)抗体和免疫球蛋白 G(IgG)抗体的检测,能够表征病毒感染的时间进程^[29-31]。

针对血清样本中的抗体检测,Santos 等^[32]开发了一种基于 SPR 与主要衣壳蛋白(VP1)关联的甲型肝炎病毒(HAV)检测工具,在检测抗 HAV 多克隆 IgM 抗体中表现了良好的性能,能够有效地表征阳性和阴性血清样本之间的显著差异,检测限(LOD)为 0.218 nmol/L。徐超等^[33]通过将鸭瘟病毒(DPV)gC 糖蛋白偶联在 SPR 传感芯片上,建立了一种特异性显著的 SPR 鸭瘟检测方法,该芯片表面的 gC 糖蛋白仅与鸭瘟阳性血清有明显反应,而与鸭流感病毒血清、番鸭细小病毒血清等为阴性反应。

由于不同病毒抗原和抗体之间的结合能力存在差异,为了保证对目标抗体有最优异的检测性能,SPR 传感器在检测病毒抗体时,需要在传感芯片表面修饰特定的抗原。Basso 等^[34]在 SPR 传感器芯片表面分别偶联上 SARS-CoV-2 刺突蛋白(S Protein)和核衣壳蛋白(N Protein),这两种修饰不同蛋白的传感器虽然都对血清样本中的 IgG 抗体表现出优异的灵敏度,并能在 10 min 内完成检测,但是偶联 S 蛋白的传感器对阳性血清样本的检测限为 $1.04 \text{ ng} \cdot \text{mm}^{-2}$,优于偶联 N 蛋白的传感器的检测限($1.34 \text{ ng} \cdot \text{mm}^{-2}$)。对于基于病毒抗原和抗体特异性结合原理的生物传感器而言,找到抗原-抗体的结合常数能够进一步优化这类传感器。Jahanshahi 等^[35]使用 SPR 技术评估 DENV 抗原和抗体之间的相互作用,正确计算了 DENV 抗原和抗体相互作用的结合常数和化学计量数据,并获得了测定 DENV 抗体样品浓度的参考曲线。

LSPR 传感器使用亚光波长的纳米粒子或结构,

能够有效定位表面等离子体激元,与 SPR 传感器相比,其在纳米粒子或结构局部具有更高的灵敏度。Funari 等^[36]在 2020 年利用电沉积技术在光微流控芯片上制备了基于 LSPR 原理的金纳米钉传感器,在微流体平台上实现了对人血中 SARS-CoV-2 刺突蛋白抗体的低浓度检测(LOD 为 0.08 ng/mL),优于商业 ELISA 在真实患者样本中的 LOD(1.6~3500 ng/mL)。Wang 等^[37]开发了基于光谱图像对比度的流动数字纳米等离子体测量法,通过对比两个选定波长带内单个金纳米颗粒(AuNP)的散射图像亮度,快速评估了 AuNP 的 LSPR 位移。该方法在检测 SARS-CoV-2 刺突蛋白的抗体时,具有 10 pg/mL 的检测限和至少 6 个数量级的动态范围。

金纳米棒(AuNRs)常作为等离子体纳米换能器在 LSPR 病毒抗体检测中得到应用,AuNRs 相对于球形 AuNPs,其额外的纵向等离子体带对周围环境的介电特性变化高度敏感,且灵敏度随着纳米棒纵横比的增加而增加^[38-40]。Versiani 等^[41]利用功能化 AuNRs 传感器对感染 DENV 的患者血清和感染寨卡病毒(ZIKV)的患者血清进行检测,其原理如图 2(a)所示。对于感染了 DENV 的患者血清,修饰 DENV1 E、DENV2 E、DENV4 E 蛋白的 LSPR 传感器都发生了超过 20 nm 的波长偏移,修饰 DENV3 E 蛋白的传感器也发生了 10 nm 的窄幅变化。而对于感染同属于黄病毒科的 ZIKV 的患者血清,AuNRs 传感器发生的波长偏移并不显著,仅为 0~2 nm,这种基于 LSPR 的金纳米棒传感器显示出了优异的特异性。

AuNRs 纳米传感器虽然具备比 AuNPs 更优异的性能,但是长时间保存于溶液中会出现“蓝移”现象,而将固定化 AuNRs 作为光学换能器的 LSPR 生物传感元件具有高稳定性^[43]。Huang 等^[42]在 ZIKV 检测

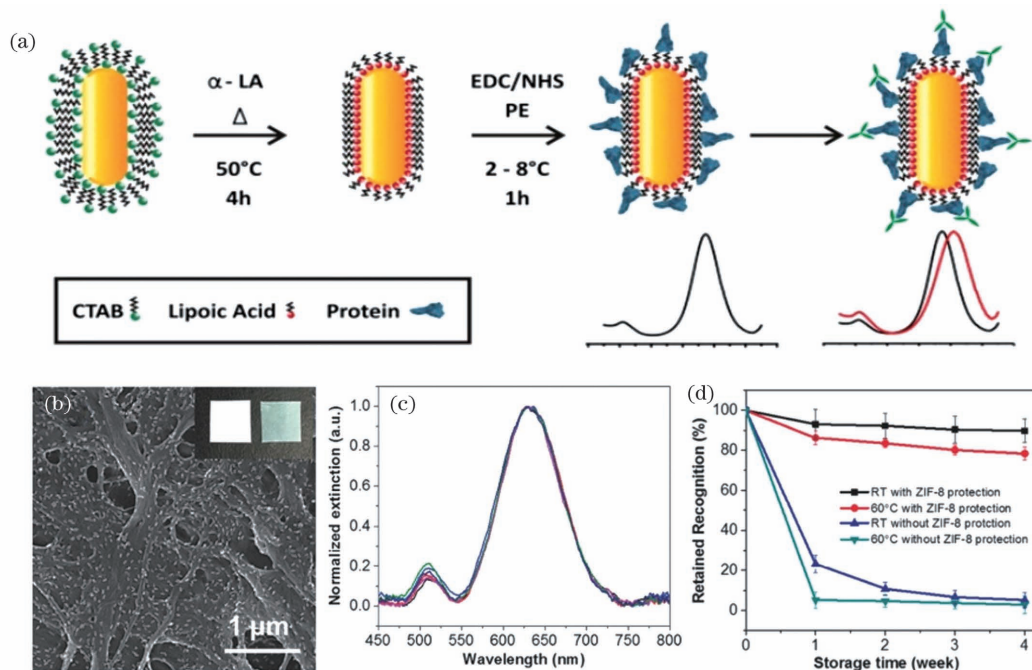


图 2 利用 AuNRs 检测病毒。(a) AuNRs 纳米传感器的检测原理^[41]；(b) 带有 AuNR-ZIKV-NS1 偶联物的滤纸的扫描电镜 (SEM) 图^[42]；(c) BPD 上不同区域采集的消光光谱^[42]；(d) 不同保存条件下 BPD 上 ZIKV-NS1 的活性变化^[42]

Fig. 2 Virus detection using AuNRs. (a) Detection principle of AuNRs nanosensor^[41]；(b) scanning electron microscopy (SEM) image of filter paper with AuNR-ZIKV-NS1 conjugate^[42]；(c) extinction spectra at different regions of BPD^[42]；(d) activity changes of ZIKV-NS1 on BPD under different storage conditions^[42]

领域开发出了一种纸基底的 LSPR 生物传感器 (BPD), 传感器表面如图 2(b) 所示, 该传感器引入纸质基底避免了 AuNRs 的变性, 引入金属有机框架 ZIF-8 避免了传感器中修饰的 ZIKV 非结构性蛋白 1 (ZIKV-NS1) 失活。由图 2(c) 可见, BPD 不同区域的消光光谱十分均匀, 纸基底不会引起系统误差。在图 2(d) 中, BPD 在室温 (RT) 和 60 °C 环境中保存 4 周, 保留了近 89% 和 78% 的识别能力。这种纸基底 LSPR 传感器对血清中 IgG 抗体的 LOD 为 200 ng/mL, 在磷酸缓冲盐溶液 (PBS) 中 LOD 为 1 ng/mL, 检测限的差距可能来源于血清中其他生物介质对传感器的污染。

3 SPR/LSPR 传感器检测病毒抗原

SPR 和 LSPR 传感器检测病毒抗原与抗体都是基于抗原-抗体特异性结合的免疫学原理, 抗原检测是将抗体或适体修饰在 SPR 或 LSPR 传感器表面。病毒抗原是带有病毒基因编码的特殊蛋白质, 病毒复制时产生大量蛋白质抗原^[44], 此时大量抗体-抗原复合体在宿主体内生成, 导致生物体液中的抗体数量急剧减少, 因此抗体检测将存在“窗口期”, 抗原检测是缩短“窗口期”的方法之一^[45-46]。

HIV 宿主在“窗口期”内具有传染性, 而 HIV 抗体在“窗口期”内可能无法被检测到, 对血清中 HIV p24 抗原的检测通常在感染后 4~11 d 内就能进行^[47]。Sarcina 等^[48]首次使用物理和化学两种方式固定 HIV-1 p24 衣壳蛋白小鼠单克隆抗体, 物理固定通

过沉积作用将抗体固定在 SPR 传感器金层表面, 化学固定通过混合链烷硫醇的自组装单层 (SAM) 锚定抗体。在对 HIV-1 p24 衣壳蛋白的检测中, 物理固定的 SPR 传感器检测限达到了 $(27 \pm 1) \text{ nmol/L}$, 化学固定的 SPR 传感器的检测限低了一个数量级, 为 $(4.1 \pm 0.5) \text{ nmol/L}$, 化学固定方法对检测限的优化可能是基于 SAM 能够作为支持生物受体的防污层。

对修饰抗体进行筛选是保证传感器检测性能和特异性的关键。Sharma 等^[49]首先通过在 SPR 传感器芯片表面固定埃博拉病毒重组核蛋白 (EBOV-rNP), 对埃博拉病毒三种单克隆抗体进行了筛选, 筛选出对 EBOV-rNP 有最高亲和力的抗体 mAb3, 然后将 mAb3 抗体固定在 SPR 金芯片上, 修饰 mAb3 抗体的传感芯片能对质量浓度为 0.5 pg/mL 的 EBOV-rNP 抗原产生信号响应。同时, 他们还确定了 mAb3 和 EBOV-rNP 之间相互作用的热力学参数。

在 SPR 传感器金层表面加载二维 (2D) 材料或者含有金属氧化物纳米粒子的薄膜能进一步提高传感器性能。陆彩燕等^[50]构建的单层石墨烯/少层 $\text{Ti}_3\text{C}_2\text{T}_x\text{MXene}$ /银膜结构, 较传统角度调制的 SPR 传感结构, 增强因子提高了四个数量级。彭芳等^[51]将石墨烯连接在 SPR 传感器金层表面, 通过对不同 HIV-1 p24 抗体浓度的筛选, 确定了最佳的抗体修饰浓度, 在对 HIV-1 p24 抗原的检测中, 金层-石墨烯芯片表现出了优于传统裸金芯片的检测限, 并且石墨烯增敏的 SPR 芯片具有较好的重复性与特异性。Omar

等^[52]在 2018 年,使用旋涂法在金/Fe-MPA-NCC-CTAB/EDC-NHS 薄膜上固定登革热特异性 IgM 抗体,实现了对浓度为 0.0001~10 nmol/L 的登革 E 蛋白的检测,并且该 SPR 传感器信号角度的变化与 E 蛋白的浓度呈线性关系。2020 年,Omar 等^[53-54]比较了多种材料在金层上旋涂后 SPR 共振角的变化,最终确定了自组装单层/还原氧化石墨烯-聚酰胺-胺型树状聚合物(SAM/NH₂rGO/PAMAM)薄膜能够显著提高倏逝波的穿透深度,是 SPR 技术中最好的登革传感介质,能够在 8 min 内检测出浓度为 0.08 pmol/L 的 DENV2 E 蛋白。

基于氧化还原反应的电调制光信号策略在 SPR 传感器中较为少见,氧化还原反应可以改变生物共轭界面附近的折射率,从而提高 SPR 生物传感器的灵敏度。Qatamin 等^[55]将微电化学流动池和 SPR 传感器结合,利用 SPR 金传感芯片和二抗偶联的氧化还原活性亚甲蓝染料形成夹心结构,能够实现亚甲蓝的氧化还原控制,从而调制光信号,提高灵敏度。在 H5N1

甲型禽流感病毒的血凝素(HA)蛋白检测中,他们提出的电化学表面等离子体共振(EC-SPR)传感器的检测限为 300 pmol/L。值得注意的是,检测流感病毒 HA 蛋白需要考虑抗原漂移的影响,抗原漂移会导致 HA 与唾液酸的结合特性改变。一种新的 HA-聚糖 SPR 方法通过评估唾液酸和血凝素的结合能力来表征流感病毒的血凝素活性,在疫苗性能表征、血清样品滴度评估等领域有很好的应用前景^[56]。

SPR 传感芯片的金属膜层结构设计和优化已经得到了大量研究^[57-58],而自组装 AuNPs 代替金属层作为传感芯片的研究报道较少。Kim 等^[59]通过将 AuNPs 异质组装在载玻片表面上,制造了传感芯片,AuNPs 单层和单一 AuNP 构成免疫夹心结构,芯片和 AuNP 之间的近场电子耦合可放大 SPR 响应信号,该夹心结构对 HBsAg 的检测限比单一异质组装 AuNPs 芯片高 100 倍,在临床人血清样品中展示了 10 pg/mL~10 ng/mL 的检测范围,该传感器工作示意图如图 3 所示。

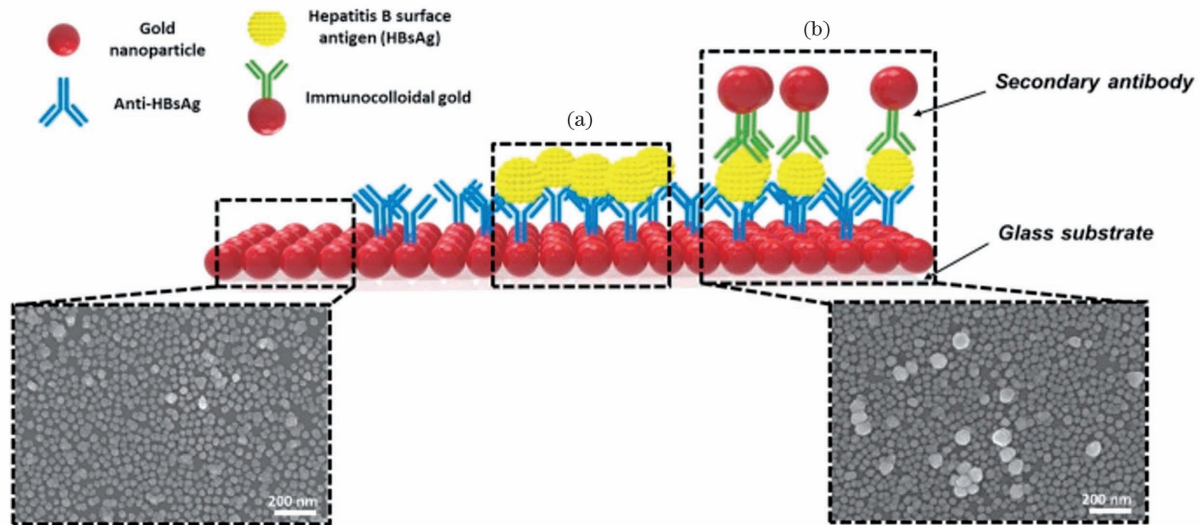


图 3 LSPR 生物传感器芯片工作示意图^[59]。(a)异质组装 AuNPs 芯片病毒检测示意图;(b)AuNPs 和异质组装 AuNPs 层夹心结构病毒检测示意图

Fig. 3 Working diagrams of LSPR biosensor chip^[59]. (a) Schematic of virus detection by heteroassembled AuNPs chip; (b) schematic of sandwich structure composed of AuNPs and heteroassembled AuNPs layer for virus detection

在此前的研究中,针对病毒的 SPR 和 LSPR 传感器多是基于抗原-抗体进行蛋白质抗原的检测,适体是对目标抗原具有高亲和力的寡核苷酸或者多肽,相比抗体,适体有成本低、重复性好等特点。Heo 等^[60]开发了一种亲和肽引导的 LSPR 生物传感器,能够在最低基本培养基(MEM)和胎牛血清(FBS)混合成的复合组织培养基中检测出浓度仅为 0.1 ng/mL 的诺如病毒衣壳蛋白,该传感器还有着优秀的特异选择性,对轮状病毒不产生任何信号响应。Lewis 等^[61]将 SARS-CoV-2 S1 刺突蛋白的特异性适体代替传统的抗体作为传感器识别元件,能特异性识别捕获 S1 刺突蛋白,但对 S2 刺突蛋白、RBD 刺突蛋白不敏感。该 LSPR 适体传感器在不同浓度的抗原蛋白流经金纳米芯

片时,表现出了极好的动态响应范围(1~100 nmol/L),在保证 0.26 nmol/L 检测限的同时,能进行高达 9 次的重复检测。同时,传感器芯片在缓冲液中的存储时间达到了三周。

Lee 等^[62]引入三路连接法(3WJ),用多功能 DNA 构建成生物探针。DNA 3WJ 探针的三个功能片段分别为 HA 结合适体、荧光素(FAM)染料和硫醇基团,适体捕获 HA 蛋白,FAM 染料增强 LSPR 效应,硫醇基团连接空心金尖峰状纳米颗粒(HAuSN),HAuSN 固定于氧化铟锡(ITO)基板上,实现了基于 LSPR 技术的无标记禽流感(AIV H5N1)HA 蛋白检测,其传感示意图如图 4 所示。生物探针在 PBS 和稀释鸡血清中都取得了 1 pmol/L 的优异检测限表现,优于一

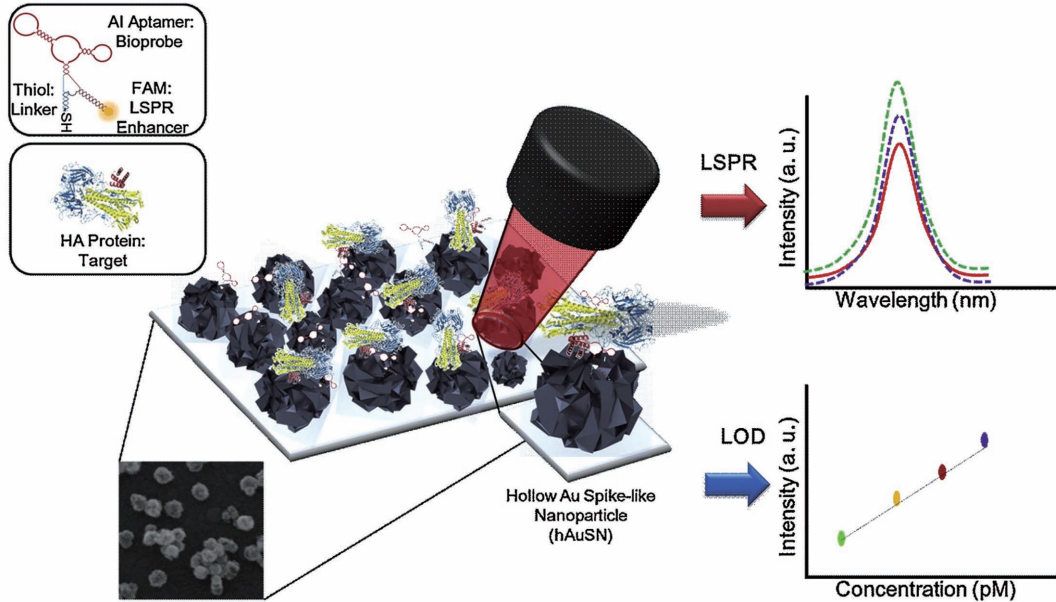


图 4 多功能 DNA 三路连接 HAuSN 传感器示意图^[62]

Fig. 4 Schematic of multi-functional DNA 3-way connected HAuSN sensor^[62]

种结合石英晶体微天平(QCM)和 SPR 的传感器对甲型流感 HA 的检测结果^[63], 并且信号强度和 HA 蛋白浓度呈线性相关。

Zang 等^[64]设计了一款 3D 纳米天线 LSPR 传感芯片, 结构如图 5(a)所示, 金盘与金层形成纳米腔增强光吸收和光发射, 柱侧的金纳米颗粒增强局域光场。此传感器将兔多克隆抗体 IgG 作为捕获抗体固定在

金盘表面, 捕获 EBOV 可溶性糖蛋白(sGP)后, 加入检测抗体(小鼠 IgG 单克隆抗体), 再添加由 IRDye800 红外荧光团标记的山羊抗小鼠 IgG 二抗, 最终形成的夹心结构可增强信号, 夹心结构的细节分解图如图 5(b)所示。该 3D 纳米天线传感芯片对人血浆的检测限为 220 fg/mL, 是现有免疫测定法检测限的 24 万倍。

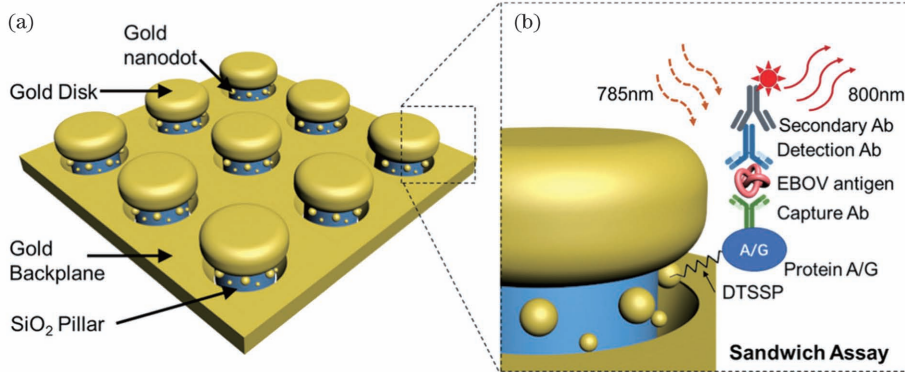


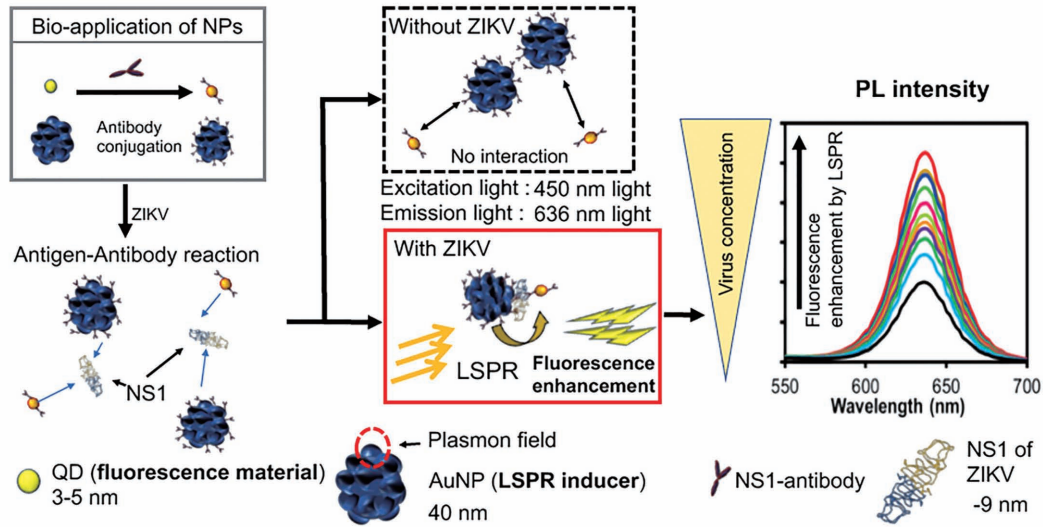
图 5 EBOV 传感器的纳米结构和荧光传感方法^[64]。(a)3D 纳米天线 LSPR 传感芯片结构图;(b)夹心结构分解图

Fig. 5 Nanostructure of EBOV sensor and fluorescence sensing method^[64]. (a) Structural diagram of 3D nano-antenna LSPR sensor chip; (b) decomposition diagram of sandwich structure

Takemura 等^[65]用 NS1 抗体修饰 AuNPs 和 CdSeTeS 荧光量子点, 用于检测寨卡病毒的非结构蛋白 1(NS1)。由于抗体-抗原之间的亲和作用, AuNPs 和荧光半导体量子点(QD)偶联在同一个抗原上, 此时来自 AuNPs 的 LSPR 信号将会对 QDs 的荧光信号进行增强, 其传感原理如图 6 所示。在检测去离子水中 NS1 时, 其具有 10 fg/mL~1 ng/mL 的宽广检测范围, 检测限为 1.28 fg/mL。此外, 他们还研究了抗体和金纳米颗粒之间不同的连接物对检测限的影响。

上述三项利用 LSPR 技术检测病毒抗原的研究都

是通过等离子体场激发荧光物质来实现 LSPR 信号增强, Lee 等^[62]和 Zang 等^[64]还通过引入等离子体纳米结构来提高传感器性能, HAuSN 和 3D 纳米天线结构具有独特的局部折射率。值得注意的是, 3D 纳米天线 LSPR 传感芯片的检测限高于 Takemura 等^[65]的传感方案, 原因可能是两项研究中样品溶液的差别, 去离子水相对于血浆而言, 不存在生物介质污染问题, 另一个原因可能是 QD 与有机染料或荧光蛋白相比, 前者的荧光效应更强, 且具备更佳的抗光漂白特性^[66]。

图 6 LSPR 放大的免疫荧光生物传感器的示意图^[65]Fig. 6 Schematic of immune-fluorescence biosensor magnified by LSPR^[65]

4 SPR/LSPR 传感器检测病毒核酸

病毒的遗传物质通常为一个核糖核酸基因组或脱氧核糖核酸基因组。遗传物质进入细胞后,遗传物质和蛋白质大量复制,直至细胞死亡后释放已经重组的新病毒^[67]。而基于核酸检测的生物传感器就是将一个单链寡核苷酸固定在传感器表面作为探针,通过捕获相对应的互补 DNA 序列来改变等离子体信号,从而实现病毒的检测^[68]。

在实际检测中,由于临床样本中病毒基因组的数量通常相当小,因此传统的 SPR 或 LSPR 传感器检测 DNA 时受到较大限制,SPR 或 LSPR 传感技术单独检测病毒核酸临床样品时表现了较差的检测限。Das 等^[69]检测金纳米颗粒的 LSPR 吸收峰时,仅能检测质量浓度在 $0.5 \mu\text{g}/\text{mL}$ 以上的辣椒卷叶病毒(ChiLCV) DNA。基于比色法开发了一款修饰反义寡核苷酸(ASOs)的金纳米颗粒传感器^[70],在检测 SARS-CoV-2 N 基因(核衣壳磷酸蛋白)等 RNA 序列时,虽然能依靠“裸眼”在 10 min 内完成对病毒 RNA 样品的检测,并证明了金纳米颗粒的 SPR 吸收光谱红移了约 40 nm,但 LOD 仅为 $0.18 \text{ ng}/\mu\text{L}$ 。

将 DNA 扩增技术和 SPR 相结合,传感器实现了飞(f)量级的目标检测,已有研究证明,其在蛋白质和 DNA 检测中具有超高的灵敏度和特异性^[71-72]。环介导等温扩增(LAMP)技术是用酶进行 DNA 扩增的技术之一。Chuang 等^[73]设计了一种结合 SPR 和 LAMP 技术的感应盒,SPR 传感器对介质折射率的变化十分敏感,而病毒 DNA 的 LAMP 扩增会导致介质的静态折射率发生变化,SPR 传感器通过特殊设计的聚碳酸酯梯形棱镜实现了在 17 min 内对不同初始浓度乙型肝炎病毒 DNA 模板的 LAMP 溶液的实时响应,LOD 低至 $2 \text{ fg}/\text{mL}$ 。PCR 扩增是另一种酶扩增技术。Lugongolo 等^[74]为了研究 SPR 传感器对 HIV 基

因组中突变基因的检测能力,使用 PCR 扩增 HIV-1 pol 基因的 174bp 区域,形成了目标 DNA 序列,利用角度偏移幅度评估了 SPR 传感器对三种样品折射率差异的反应,成功检测到了互补 DNA 探针和目标 DNA 的杂交。廖婧等^[75]使用 SPR 技术对纯化样品 PCR 扩增产物进行 HPV 基因型检测,佐证了 hTERT 基因的异常扩增和 HPV 感染率与组织病变升级相关。

在许多研究中,SPR 生物传感器检测 HIV 病毒 DNA 都是使用酶作为信号放大器^[76],LAMP 和 PCR 技术都是利用酶法扩增 DNA,但是酶对温度有严格要求,且成本高,而 DNA 纳米技术通过 DNA 链来操纵物质的空间和时间分布,能够代替酶应用,实现无酶 DNA 扩增。Diao 等^[77]开发了一种基于熵驱动链置换反应和双层 DNA 四面体(DDT)的高灵敏度、无酶、无标记的 SPR 病毒传感器,用于 HIV 相关 DNA 的检测。靶 DNA 在与发夹探针三链复合物结合后,释放出大量双链复合物(dsDNA),并引发链置换反应,在探针捕获双层 DNA 四面体并形成三层复合结构时,SPR 响应显著增长。此传感器的响应信号不仅与 DNA 浓度呈线性关系,而且同一芯片在使用 100 次后仍保持一定的检测性能,LOD 为 $48 \text{ fmol}/\text{L}$ 。

在上述基于 DNA 技术的信号放大手段中,对 DNA 进行有酶或无酶扩增能显著提高 SPR 或 LSPR 传感器的灵敏度^[78],图 7 罗列了几种常用的扩增技术。基于酶的 DNA 扩增技术除了 LAMP 扩增和 PCR 扩增,还包括指数扩增反应(EXPAR)^[71]、滚环扩增(RCA)^[79]、聚合延伸反应(PER)^[80]和连接链反应(LCR)^[81]等,这些基于酶的扩增技术具有快速、特异性高的优点。无酶 DNA 扩增技术包括杂交链反应(HCR)和催化发夹组装(CHA),HCR 技术展示了利用未修饰的单链 DNA 构建生物传感器的可行性,而由 DNA 纳米技术发展来的 CHA 技术能够放大和转导核酸扩增反应末端信号。

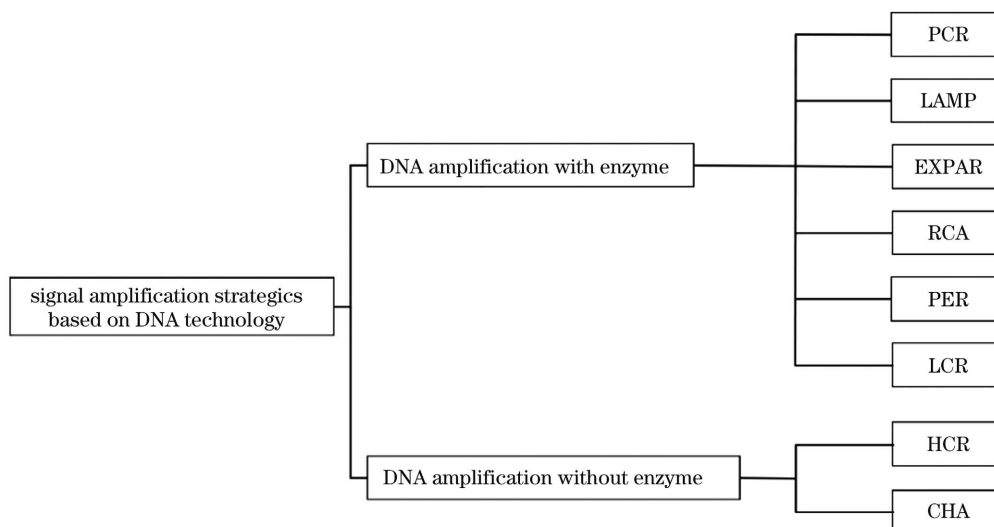
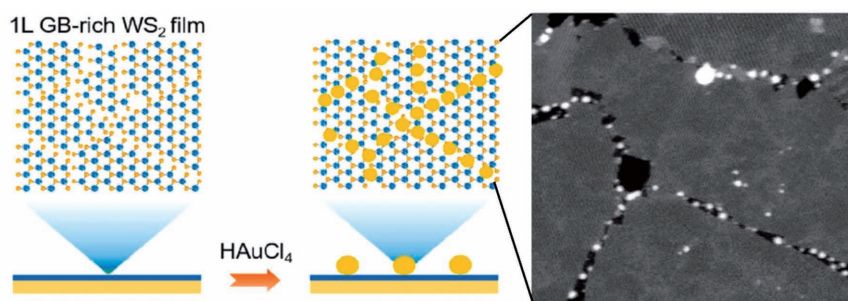


图 7 使用 DNA 技术的用酶、无酶扩增手段

Fig. 7 Enzymatic or non-enzymatic amplification using DNA technique

除了 DNA 扩增技术,石墨烯、 MoS_2 、 WS_2 等 2D 材料的出现为 SPR 传感器性能的提升提供了新的方向,其具备层状结构、高表面积体积比等特点,在大量研究中使用 2D 材料的 SPR 传感器的灵敏度优于裸金层 SPR 传感器^[51,82]。在病毒核酸检测领域,研究者提出了一种将石墨烯基多层涂层沉积在金层表面的 SPR 传感器优化模型,对其设计模型、制造工艺等方面进行了说明,同时对 SARS-CoV-2 病毒产物(抗体、抗原、核酸)检测进行了模拟,证明了模型的可行

性^[83]。而 Liu 等^[84]通过在金层表面制备晶圆级多晶单层 $\text{W}(\text{Mo})\text{S}_2$ 薄膜,在薄膜的晶界(GB)结构缺陷处还原了溶液中的 AuCl_4^- 离子,实现了 AuNPs 在 GB 缺陷处的原位生长,如图 8 所示,并将互补 DNA (cDNA) 偶联于 AuNPs 表面,完成了浓度低至 0.1 fmol/L 的 SARS-CoV-2 病毒的 RNA 序列检测。利用结构缺陷原位生长 AuNPs 以弥补 2D 材料难以固定生物受体的缺点,是基于 2D 材料的 SPR 生物传感器的发展方向之一。

图 8 富含 GB 的 $\text{W}(\text{Mo})\text{S}_2$ 薄膜的 AuNPs 改性及其 SEM 图^[84]Fig. 8 AuNPs modification of $\text{W}(\text{Mo})\text{S}_2$ film rich in GB and its SEM diagram^[84]

将 SPR 或 LSPR 技术与荧光物质、光热效应结合也能在一定程度上提升传感器的检测限。Chowdhury 等^[85]构建了基于四种血清型 DENV 的夹型单链 DNA(ssDNA)连接的 ssDNA-CdSeTeS QDs 探针,通过 DENV 的互补 DNA/RNA 和靶 ssDNA 的杂交,打开了探针发夹结构,留出了互补空位,游离的功能化 AuNPs 在探针空位互补结合,对 QDs 产生增强或淬灭效应,实现了对四种 DENV 血清型的检测,原理如图 9(a)所示,其 LOD 分别为 24.6, 11.4, 39.8, 39.7 fmol/L。QDs 荧光强度与金属纳米颗粒的粒径、材料结构有关,为了获得最优的荧光效应,需要对纳米颗粒进行优化。Adegoke 等^[86]为了检测 ZIKV,设计了四种等离子体纳米颗粒-荧光量子点-分

子信标(NP-QD-MB)生物传感器,如图 9(b)所示,其中双金属等离子体纳米颗粒和荧光半导体量子点的组合能够激发更强的 LSPR 介导荧光信号,表现最优的 AuAg 合金 NP-Qdot646-MB 传感器能对病毒载量为 1.7 copy/mL 的病毒 RNA 作出响应。

Qiu 等^[87]将 LSPR 技术和等离子体光热效应(PPT)结合,构建了一种基于功能化二维金纳米岛(AuNI)检测 SARS-CoV-2 病毒特定核酸的光热辅助等离子体传感(PTAPS)方法,PPT 效应可以显著改善 RdRp-COVID 序列及其 cDNA 配体的杂交动力学和核酸检测的特异性,双功能金纳米岛传感器的检测下限为 0.22 pmol/L。2021 年,Qiu 等^[88]引入了新的热等离子体辅助双模式转导(TP-DMT)概念,将无扩增直接

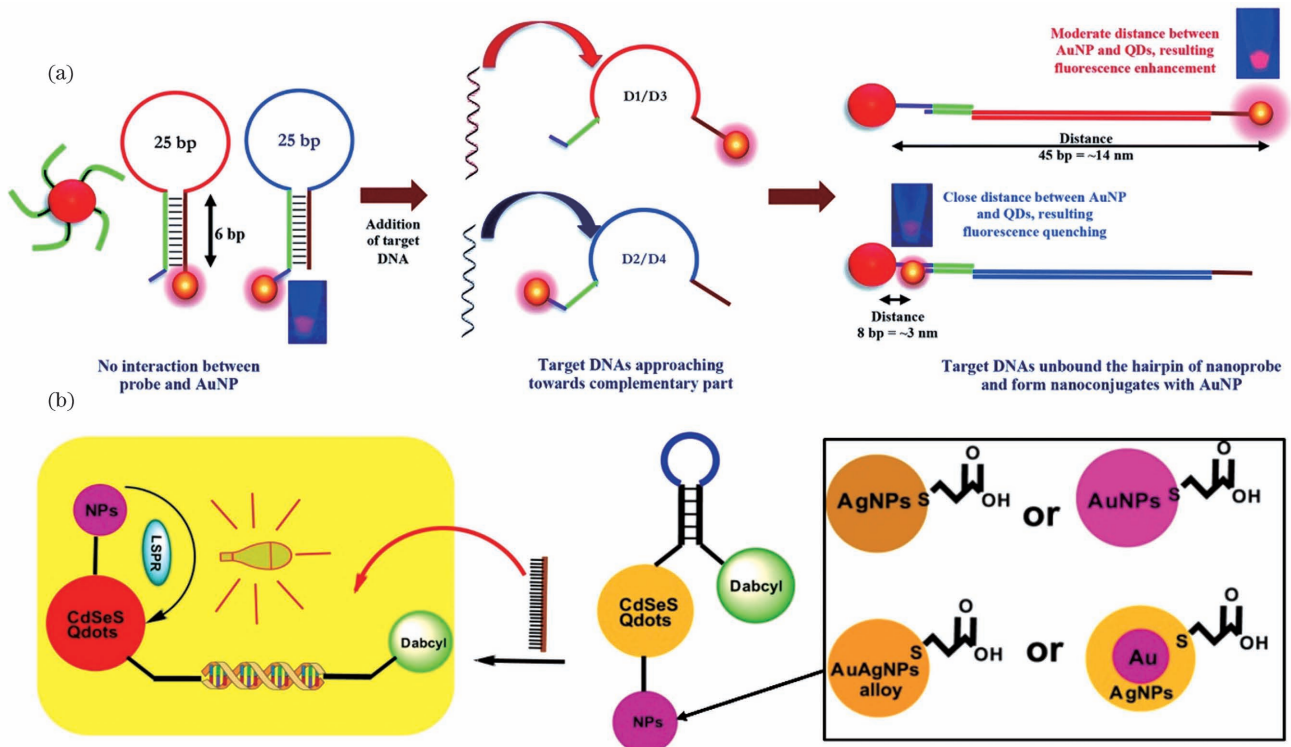


图 9 LSPR 结合 QDs 增强灵敏度。(a)利用 AuNPs 和发夹 ssDNA-CdSeTeS QDs 检测 DENV 的机制示意图^[85]; (b)四种 NP-Qdot-MB 生物传感器探针检测 ZIKV 的示意图^[86]

Fig. 9 LSPR combined with QDs to enhance sensitivity. (a) Mechanism diagrams of DENV detection using AuNPs and hairpin ssDNA-CdSeTeS QDs^[85]; (b) schematics of four NP-Qdot-MB biosensor probes for ZIKV detection^[86]

病毒 RNA 检测和循环荧光探针裂解(CFPC)结合,实现了双功能金纳米岛 LSPR 传感,该 TP-DMT 传感系统能在 30 min 内对目标病毒的核酸序列进行量化检测。这种双模式具备更高的可靠性,直接检测时检测限达到了 $(0.1 \pm 0.04) \text{ pmol/L}$,在经过 CFPC 后检测限提高了三个量级,为 $(0.275 \pm 0.051) \text{ fmol/L}$,较此前的研究取得了极大的提高。

5 SPR/LSPR 传感器检测病毒颗粒

病毒蛋白抗原和病毒核酸的检测都需要从病毒中分离目标物或者在血清中对目标物进行纯化处理,而病毒颗粒的直接检测可以缩短样品的前处理时间。病毒颗粒的捕获在大多数 SPR 和 LSPR 生物传感器中仍是依赖抗原-抗体/配体-分析物的特异性结合原理^[89-92],值得注意的是,在 Wang 等^[93]的研究中,甲型 H1N1 流行性感冒病毒颗粒可以在无修饰的金层实现黏连,病毒颗粒-金层的连接表现出了比病毒颗粒-抗体偶联体更强的稳定性。

2018 年,Chang 等^[94]通过小鼠免疫系统制备了特定的抗 HA7 单克隆抗体(Auti-HA7 mAb),这种抗体经 ELISA 评估后展现了比两种市售单克隆抗体(mAb)更高的 H7N9 病毒检测能力。在强度调制型 SPR 传感器芯片表面修饰 Auti-HA7 mAb 后,对 PBS 稀释的 H7N9 病毒的检测限为 144 copy/mL,对鼻黏膜分泌物稀释的 H7N9 病毒的检测限为 402 copy/mL。

AuNPs 扩增夹心免疫传感是一种粒子增强型 SPR 免疫传感结构,金层表面抗体捕获分析物后,二抗修饰的 AuNPs 连接到分析物,形成了夹心结构,从而显著增强了 SPR 信号。AuNPs 和金层之间的电磁场耦合,以及 AuNPs 通过增加分析物质量来提高 SPR 表面折射率,这两点被认为是 SPR 信号增强的原因^[95-96]。Das 等^[97]提出了一种金层-病毒-金纳米棒夹心结构的等离子体传感器模型,在金层和 AuNRs 表面修饰 SARS-CoV-2 刺突蛋白抗体,金层经修饰物与 SARS-CoV-2 病毒表面的刺突蛋白实现偶联,捕获病毒颗粒,然后添加 AuNRs 产生夹心复合体结构,如图 10(a)所示。在模拟中 AuNRs 能够显著放大电场,同时 AuNRs 的纵横比以及与金层的距离也是改善电场的关键因素。Huang 等^[98]通过实验,在金纳米杯状阵列传感器芯片表面使用 SARS-CoV-2 刺突 mAb 捕获 SARS-CoV-2 假病毒,并用功能化的金纳米颗粒连接病毒,形成金杯阵列-病毒-金纳米颗粒的夹心结构,如图 10(b)所示,这种双抗体夹心等离子体共振免疫测定法不仅可以扩大检测范围,还可以提高检测特异性。

分子印迹聚合物(MIP)作为生物传感器的识别元件已得到广泛运用,如噬菌体 MS2 检测^[99],MIP 相比于抗体具备更优异的稳定性和可重复性^[100]。Cennamo 等^[101]提出了一种将 SPR 光纤传感器与 MIP 技术结合的 SARS-CoV-2 病毒颗粒检测方法,这种 SPR-POF-MIP 传感器通过在含有 60 nm 厚金层的

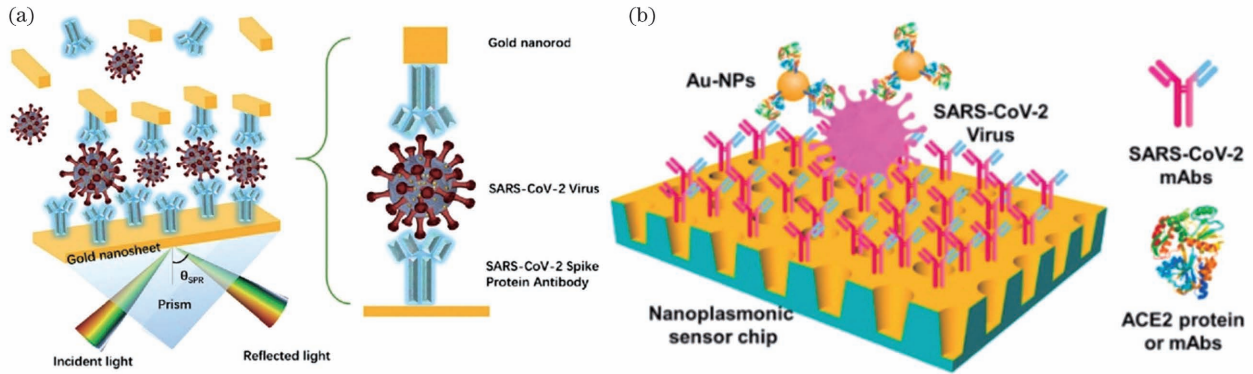


图 10 夹心结构传感器。(a) 金层-病毒-金纳米棒夹心结构等离子体传感器^[97]；(b) 金杯阵列-病毒-金纳米颗粒的夹心结构等

离子体传感器^[98]
Fig. 10 Sensors with sandwich structure. (a) Plasma sensor with gold layer-virus-gold nanorod sandwich structure^[97] ;
(b) plasma sensor with gold cup array-virus-gold nanoparticle sandwich structure^[98]

D 型塑料光纤 (POF) 上合成 MIP 纳米层, 实现对 SARS-CoV-2 病毒颗粒的捕获, 在检测阴性和阳性鼻咽拭子样品时, SPR-POF-MIP 对生理溶液中阳性样品的检测限远远小于逆转录聚合酶链式反应 (RT-PCR)。光纤 SPR 传感器的改进策略除了分子印迹外, 还可以考虑从纤维基材、本征层 (金属层) 和表面纳米材料改性等方面进行优化, 从而提高传感器灵敏度、可靠性等性能指标^[102-103]。

利用 LSPR 对荧光半导体量子点的荧光增强或淬灭效应来提高病毒传感器的灵敏度已有较多应用, 如 V 型 SPR 传感器检测诺如病毒颗粒^[104]、LSPCF-FOB 传感器检测猪源甲型流感病毒 (S-OIV)^[105] 等。QD 的荧光强度与 AuNPs 的浓度、大小和距离有关, 即使

在检测极低浓度的病毒时, 传感器捕获到病毒也会导致 AuNP-QD 复合体微纳结构发生变化, 从而使得荧光强度发生剧烈变化。

近年来, 日本研究团队通过结合 AuNPs 与 QDs 来检测病毒颗粒。2017 年, Takemura 等^[106] 通过在 AuNPs 和 CdSeTeS 合金核量子点粒子表面分别修饰抗神经氨酸酶 (NA) 抗体和抗血凝素 (HA) 抗体, 实现了两种粒子在病毒表面的偶联, 病毒表面 AuNPs 诱导的 LSPR 效应增强了相邻 QDs 的荧光强度, 如图 11(a) 所示, 荧光强度与目标病毒浓度变化成正比, 从而实现了质量浓度低至 0.03 pg/mL 的 H1N1 病毒的检测, 并在 H3N2 和诺如病毒检测中也取得了较好效果。

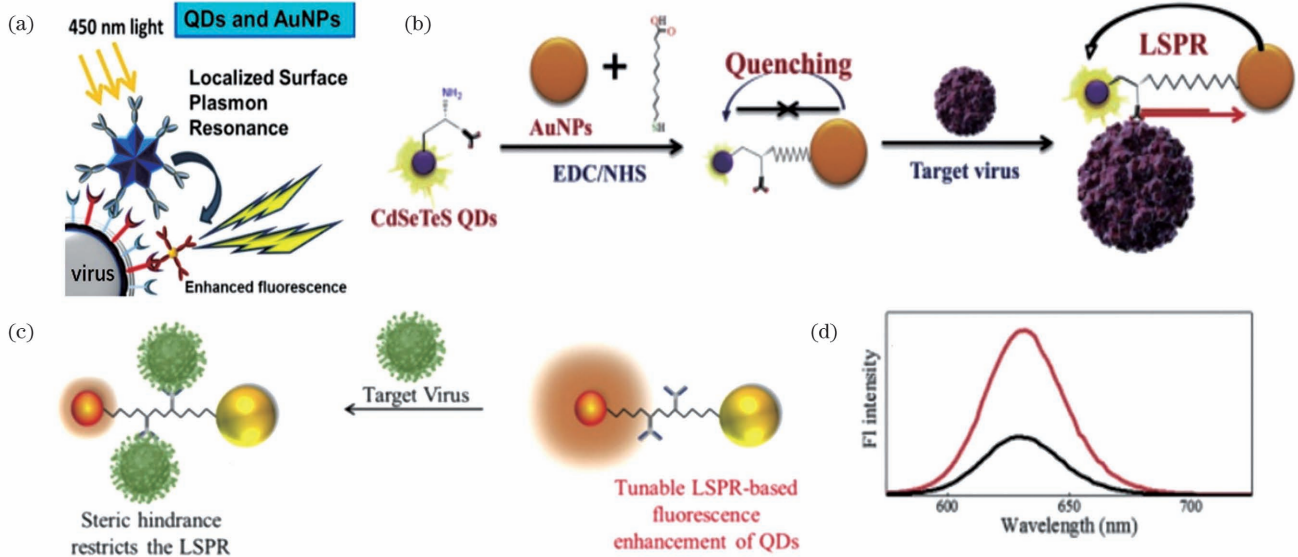


图 11 金纳米颗粒-荧光量子点传感探针。(a) AuNPs 的 LSPR 效应增强相邻 QDs 荧光强度的示意图^[106]；(b) CdSeTeS QDs/AuNPs 刚性传感探针的病毒检测机理^[107]；(c) 中间连接肽长度可调节的传感探针的病毒检测机理^[108]；(d) CdZnSeS/ZnSeS QD-peptide-AuNP 传感器捕获病毒后 QD 发生的荧光猝灭^[108]

Fig. 11 AuNP-QD sensing probe. (a) Schematic of fluorescence intensity of adjacent QDs enhanced by LSPR effect of AuNPs^[106] ; (b) mechanism of virus detection using CdSeTeS QDs/AuNPs rigid sensing probe^[107] ; (c) mechanism of virus detection with adjustable length of intermediate junction peptide^[108] ; (d) fluorescence quenching of QDs after virus captured by CdZnSeS/ZnSeS QD-peptide-AuNP sensor^[108]

2018 年, Nasrin 等^[107]在 Takemura 等^[106]的工作基础上,使用抗 Nov 抗体共价连接 CdSeTeS 量子点与金纳米颗粒,制备了 CdSeTeS QDs/AuNPs 刚性传感探针,完成了质量浓度低至 12.1×10^{-15} g/mL 的诺如病毒颗粒的检测。刚性探针避免了 AuNP 和 QD 在病毒颗粒上随机连接造成的背景荧光信号过强问题。其检测原理如图 11(b)所示,传感器捕获病毒颗粒后在 QD 和 AuNP 之间产生了空间位阻,引发了淬灭荧光的再生,此传感器在临床样品上取得了比 ELISA 高 100 倍的检测限。2020 年, Nasrin 等^[108]使用肽代替原先刚性传感器的中间连接抗体,调节肽的长度使得 QD 和 AuNP 之间的距离可调,进而荧光效应得到最优化。在对 H1N1 流行性感冒病毒颗粒的

检测中,如图 11(c)、(d)所示,病毒的捕获导致了荧光的淬灭,所构建的 CdZnSeS/ZnSeS QD-peptide-AuNP 探针在性能上超越了其他基于 LSPR 的流感检测方法。Chowdhury 等^[109]详细研究了 Nasrin 等^[108]对 QD-peptide-AuNP 探针的优化工作,通过改变 AuNPs 的大小和肽的长度构建出了 36 种纳米结构,如图 12(a)~(f)所示,并对 36 种结构的荧光增强或淬灭进行了总结和分析。为了研究 AuNPs 浓度对探针的影响,将 AuNPs 的尺寸固定为 35 nm,结果如图 12(g)所示,随着 AuNPs 浓度的增加,荧光淬灭效应增强,这可能是由于 QDs 非特异性吸附 AuNPs 表面的几率增加了。优化后的结构最终在 H1N1 流行性感冒病毒颗粒、诺如病毒颗粒的检测中得到应用^[109]。

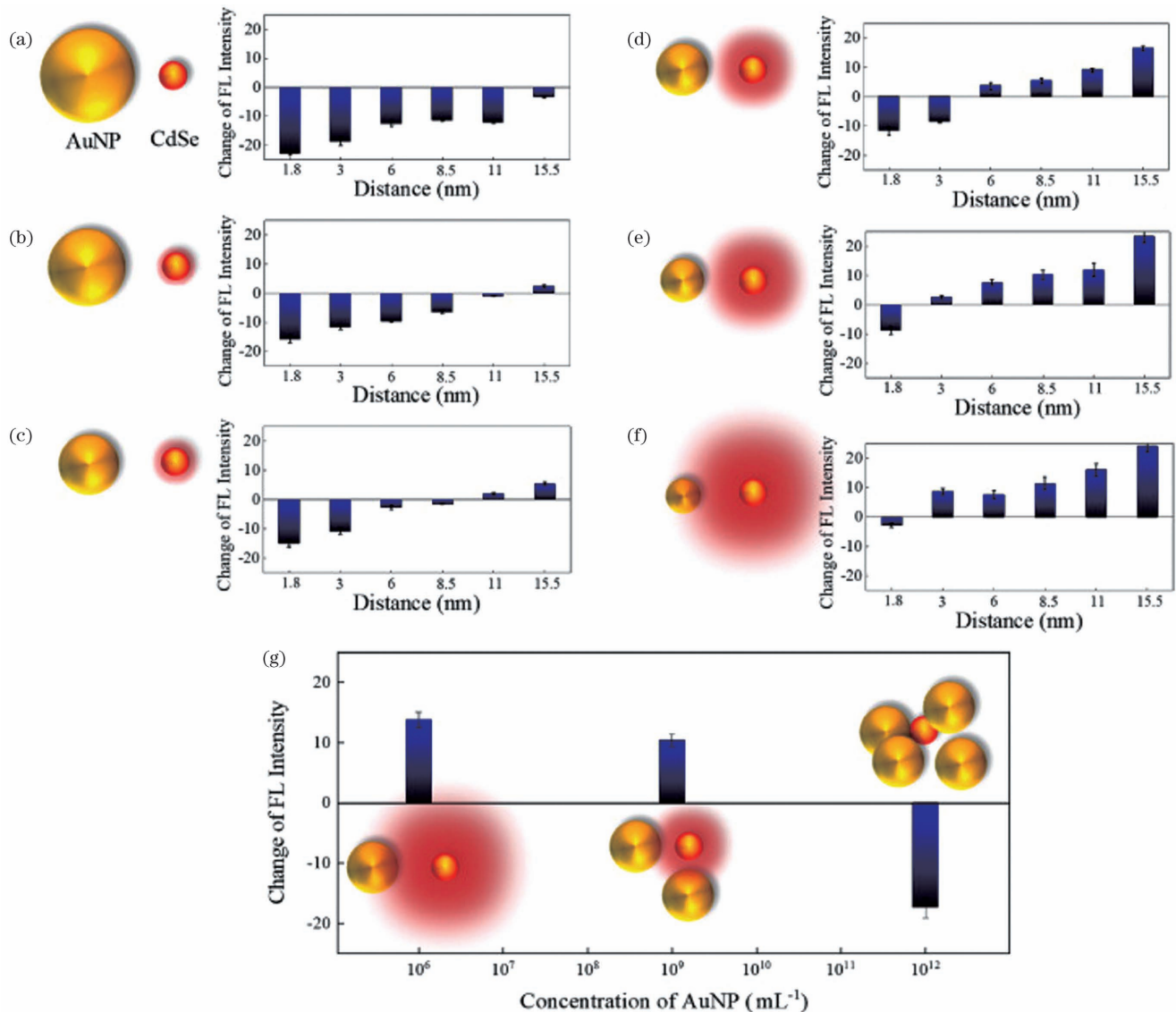


图 12 各种 CdSe QD-peptide-AuNP 纳米缀合物中 CdSe QD 的荧光光谱条形图^[109]。尺寸为(a) 80 nm, (b) 60 nm, (c) 45 nm, (d) 35 nm, (e) 25 nm 和(f) 15 nm 的 AuNPs 与六种不同长度肽相结合,产生了不同的荧光强度变化;(g)浓度为 10^{12} , 10^9 , 10^6 mL⁻¹ 的 AuNPs 对其他参数恒定的纳米缀合物的影响

Fig. 12 Fluorescence spectral bar diagrams of CdSe QDs in various CdSe QD-peptide-AuNP nano-conjugates^[109]. AuNPs with six different sizes of (a) 80 nm, (b) 60 nm, (c) 45 nm, (d) 35 nm, (e) 25 nm, and (f) 15 nm combined with peptide with six different lengths to produce different fluorescence intensity changes; (g) effect of AuNPs with concentrations of 10^{12} , 10^9 , and 10^6 mL⁻¹ on nano-conjugates with other constant parameters

6 传感器防污性与重复性

SPR 或 LSPR 生物传感器要从实验室进入临床,用于临床病毒样本的检测,亟须解决生物介质污染、重复性差等难题。利用 SAM 化学固定识别元件,能够在一定程度上缓解生物介质污染导致的传感元件性能下降的压力^[48],但 SAM 防污能力比较有限,仅限于检测缓冲溶液或掺有分析物的稀释介质^[110]。对于复杂临床病毒样品,Riedel 等^[111]通过在 SPR 传感器表面金层合成具有抗污性能的聚合物刷,如图 13(a)所示,有效减少甚至完全抑制了血浆和血清的污染,聚合物刷修饰乙型肝炎病毒表面抗原(HBsAg)后,也不

会影响抗污能力,且对 HBsAg 抗体的检测范围超过了 ELISA。

为了构建一款能重复使用且不降低传感信号强度的 SPR 传感器,Yoo 等^[112]创新性地传统 SPR 传感器的基础上利用磁场捕获抗体修饰的磁性颗粒,金层表面的磁性图案使得外部的强磁场偏转,保证磁珠不会在传感器表面聚集成团,如图 13(b)所示。通过控制磁场来更换磁性颗粒,能够保证多次测量后传感信号稳定,避免了为洗脱捕获物而对传感器进行化学处理导致的传感器性能下降^[113],如图 13(c)所示。磁性颗粒 SPR 传感器对质量浓度为 30 ng/mL~10 μg/mL 的 H1N1 流感病毒核蛋白(NP)都能够实现灵敏检测。

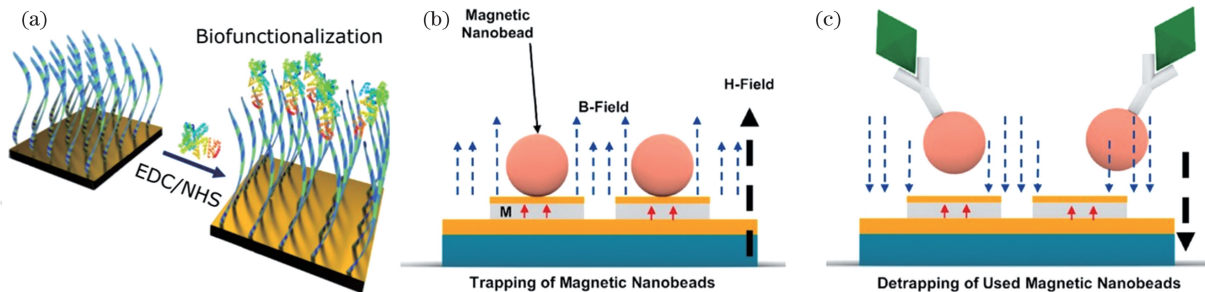


图 13 传感器防污与重复使用方案。(a)聚合物刷修饰蛋白质示意图^[111]; (b)利用外部磁场在可重复使用的 SPR 芯片上捕获磁性粒子^[112]; (c)利用与捕获方向相反的外部磁场去除磁性粒子^[112]

Fig. 13 Sensor antifouling and reuse scheme. (a) Schematic of protein modified by polymer brush^[111]; (b) trapping of magnetic particles on reusable SPR chip through external magnetic field^[112]; (c) removal of magnetic particles by external magnetic field opposite to trapping direction^[112]

7 SPR/LSPR 传感器配置及参数

表 1 罗列了近 15 年基于 SPR 或 LSPR 技术检测病毒的传感器配置及参数,可以看出:1) SPR 和 LSPR 传感器由于修饰物的多样性,能够根据病毒感染进程对不同靶物质进行针对性检测,这种灵活性是 ELISA 和 PCR 检测所不具备的;2)与 ELISA 和 PCR 动辄几个小时的检测时间相比,SPR 和 LSPR 传感器在几十分钟内即可完成病毒的检测工作;3)从 LOD 数据可以看出,SPR 和 LSPR 传感器的检测性能已经不亚于 ELISA 和 PCR 技术,在某些研究^[12, 36, 101, 107, 111]中甚至超过了 ELISA 和 PCR;4)由于使用纳米粒子的 LSPR 传感只需要光源和检测器,LSPR 技术相比于 SPR 更容易构建便携化、小型化的检测系统;5)SPR 和 LSPR 传感器在抗体检测方面的研究更加符合临床情况,其检测样本多为血清而非缓冲液。

8 总结和展望

就目前的研究进展来看,基于抗原-抗体特异性结合原理的 SPR 或 LSPR 传感器的研究重心在抗原或抗体修饰物的筛选、抗原和抗体结合能力的评估以及抗体修饰物的替代等方面。在大量研究中,研究人员意图寻找针对某种病毒检测的最优识别元件,以提高

传感器的检测性能、降低成本、增加可重复性等。传统 SPR 或 LSPR 传感器对临床病毒核酸样本的检测效果并不理想,需要结合 DNA 扩增、荧光物质等增益手段才能实现低浓度核酸样本的检测。对于优化策略,SPR 传感器主要聚焦于膜层材料增敏和金属粒子耦合增敏。膜层材料增敏包括使用 2D 材料、异质组装 AuNPs 层和分子印迹等,通过表面薄膜的构建增强实用性和适用性;粒子耦合增敏则是利用金属颗粒与金层形成的夹心结构增强 SPR 信号。LSPR 传感器的优化策略的重心则是 AuNPs、AuNRs 等纳米粒子或纳米结构的设计和优化,常结合 QD 等荧光物质形成探针,通过光吸收峰偏移或荧光光强变化检测病毒。此外,聚合物刷和可替换磁珠能够有效解决传感器生物介质污染和重复性差等问题。

SPR 和 LSPR 传感器在目标选择灵活性、检测时间及检测限方面较 ELISA 和 PCR 存在一定优势。但是 SPR 和 LSPR 技术的临床化和产业化仍面临一些挑战。首先需要考虑传感器整体的小型化和便携化;其次,要解决传感器芯片的保存问题;最后,需要降低传感器芯片的成本。可以预见,由于 SPR 和 LSPR 病毒传感器修饰物的多样性,未来或许可以通过传感器识别元件的集成化同时针对多种目标分析物进行特定病毒检测,在短时间内多维度评估病毒的感染情况,避免假阴性和假阳性案例的出现。

表 1 基于 SPR 或 LSPR 的病毒检测生物传感器
Table 1 SPR or LSPR based biosensor for virus detection

Method of detection	Sensor configuration	Technique	Capture element	Virus	Virus target	Sample solution	LOD	Time	Ref
Detect antibody	Au film	SPR	HBsAg	HBV	Anti-HBsAg Ab	HBS-EP buffer	0.00098 mg/L	-	[12]
	Au film	SPR	gC protein	DPV	DPV Ab	HBS	-	-	[33]
	Au film	SPR	DENV2 Ag	DENV2	IgM	Serum	2.125 pmol/L	-	[35]
	Au film	SPR	SARS-CoV-2 S protein SARS-CoV-2 N protein	SARS-CoV-2	IgG	Serum	1.04 ng·mm ⁻² 1.34 ng·mm ⁻²	10 min	[34]
	Au film	SPR	VP1	HAV	IgM	Serum	0.218 nmol/L	-	[32]
	Au nanospike	LSPR	SARS-CoV-2 S protein	SARS-CoV-2	Anti-SARS-CoV-2 S Ab	Serum	0.08 ng/mL	30 min	[36]
	AuNPs	LSPR	S protein	SARS-CoV-2	Anti-S mAb	S. B.	10 pg/mL	15 min	[37]
	AuNRs	LSPR	DENV1-4 E protein	DENV	Anti-DENV mAb	Serum	1 pg	-	[41]
	AuNRs	LSPR	ZIKV NSI	ZIKV	Anti-ZIKV NSI IgG	Serum PBS	200 ng/mL 1 ng/mL	-	[42]
	Au film	SPR	HBsAg	HBV	Anti-HBsAg Ab	Serum	<0.002 IU/mL	10 min	[111]
	Au film	SPR	EBV Ag	EBV	Anti-EBV Ab	Serum	-	30 min	[110]
	Au film	SPR	PHEMAT film	HBV	HBsAb	Serum	208.2 mIU/mL	30 min	[114]
	Gold capped nanoparticle array	LSPR	GBP	AIV	Anti-AI Ab	Carbonate buffer	1 pg/mL	-	[115]
	Au film	SPR	DENV Ag	DENV	IgM	Serum	-	10 min	[116]
	Au nanohole arrays	LSPR	PA	Anthrax toxin	14B7 scFv Ab	-	1 nmol/L	800 s	[117]
	Au film	SPR	Ag-BSA conjugate	DENV	IgM Ab	PBS	-	15 min	[118]
	Au film	SPR	Proteins	H5N1	H5N1 Ab	PBS	193.3 ng/mL	30 min	[119]
	Au film	SPR	HA proteins	H1N1, H3N2, B	Ab	Serum	<0.5 μg/mL	1-2 h	[120]

续表

Method of detection	Sensor configuration	Technique	Capture element	Virus	Virus target	Sample solution	LOD	Time	Ref
Detect antigen	Au film	SPR	Anti-HIV-1 p24 mouse monoclonal antibodies	HIV	HIV-1 p24 protein	PBS	Physisorbed: (27 ± 1) nmol/L Chemical: (4.1 ± 0.5) nmol/L	-	[48]
	Au film- magnetic particles	SPR	Anti-NP Ab	H1N1	H1N1 NP	PBS	30 ng/mL	~25 min	[112]
	Au film	SPR	EBOV mAb3	EBOV	EBOV-rNP	PBS	0.5 pg/mL	-	[49]
	Au film-graphene	SPR	HIV-1 p24 Ab	HIV	HIV-1 p24 Ag	PBS	10 ng/mL	-	[51]
	Au film	SPR	IgM	DENV	DENV E protein	PBS	0.0001 nmol/L	-	[52]
	Au film	SPR	DENV2 E IgM	DENV	DENV2 E protein	PBS	0.08 pmol/L	8 min	[53]
	Au film	SPR	DENV3 E IgM	DENV	DENV3 E protein	PBS	0.08 pmol/L	8 min	[54]
	Au film/ electrode	SPR	Anti-H5N1 Ab	H5N1	HA protein	-	300 pmol/L	-	[55]
	AuNPs monolayer								
	AuNPs monolayer / AuNPs	LSPR	Anti-HBsAg	HBV	HBsAg	PBS PBS Serum	10 pg/mL 100 fg/mL 10 pg/mL	10-15 min	[59]
	Glass-AuNPs	LSPR	NV binding peptides	NV	NV capsid proteins	MEM and FBS	0.1 ng/mL	-	[60]
	Glass-AuNPs	LSPR	S1 aptamer	SARS-CoV-2	S1 protein	Buffer	0.26 nmol/L	-	[61]
	ITO-HAuNPs	LSPR	DNA 3WJ bioprobe	AIV H5N1	HA protein	PBS Chicken serum	1 pmol/L 1 pmol/L	10 min	[62]
	Au film	SPR	HA protein	Influenza A	HA protein	Deionized water	0.72 μ g/mL	30 min	[63]
3D nanoantenna arrays		LSPR	IgG	EBOV	EBOV sGP	Plasma	220 fg/mL	-	[64]
AuNPs/CdSeTeS QDs		LSPR	Anti-NS1 Ab	ZIKV	ZIKV NS1	Deionized water	1.28 fg/mL	-	[65]
Optic fiber/AuNPs		LSPR	A-H1 Ab	S-OIV	rHA protein	PBS	13.9 pg/mL	-	[105]
	AuNRs	LSPR	HBsAb	HBV	HBsAg	Tris buffers	0.01 IU/mL	-	[121]
	Au film	SPR	Anti-PB1-F2 Ab	H1N1	PB1-F2 polypeptide	-	10 nmol/L	10 min	[122]

续表

Method of detection	Sensor configuration	Technique	Capture element	Virus	Virus target	Sample solution	LOD	Time	Ref
Detect nucleic acid	Au film	SPR	-	HBV	HBV DNA templates	-	2 fg/mL	17 min	[73]
	Au film	SPR	Biotinylated DNA	HIV	HIV-1 pol 174bp	PBS	-	-	[74]
	Au film	SPR	Hairpin probes/DDIT	HIV	HIV DNA	TE	48 fmol/L	60 min	[77]
	AuNPs	LSPR	ChiLCV 862BM R	ChiLCV	ChiLCV ssDNA	TE	1.0 $\mu\text{g/mL}$	10 min	[69]
	AuNPs	LSPR	ASOs	SARS-CoV-2	SARS-CoV-2 RNA	-	0.18 ng/ μL	10 min	[70]
AgNP-Qdot646-MB AuNP-Qdot646-MB Au/AgNP-Qdot646-MB AuAgNP-Qdot646-MB	AuNP-ssDNA-QD	LSPR	DENV1-4 hairpin ssDNA	DENV	Complementary ssDNA	DEPC	DENV1: 24.6 fmol/L DENV2: 11.4 fmol/L DENV3: 39.8 fmol/L DENV4: 39.7 fmol/L	-	[85]
	AuNP-Qdot646-MB	LSPR	MB	ZIKV	ZIKV RNA	-	7.6 copy/mL 2.9 copy/mL 2.4 copy/mL 1.7 copy/mL	-	[86]
	AuNI	LSPR	Thiol-cDNA	SARS-CoV-2	RdRp-COVID	-	0.22 pmol/L	-	[87]
	AuNI	LSPR	Thiol-cDNA CFP	SARS-CoV-2	SARS-CoV-2 NA	Nuclease-free water	(0.1 \pm 0.04) pmol/L (0.275 \pm 0.051) fmol/L	30 min	[88]
Au-W(Mo)S ₂ film-AuNPs	Au film	SPR	cDNA	SARS-CoV-2	RNA	PBS	0.1 fmol/L	-	[84]
	Au film	SPR	Capture probe(C1)	AIV	AI-DNA	Deionized water	0.46 $\mu\text{mol/L}$	-	[68]
	Au film	SPR	BSMV oligonucleotide	BSMV	BSMV RNA	MgCl ₂ + EDTA	14.7 pg/ μL	50 min	[123]
	Au film	SPR	RNase H	H1N1	MicroRNA miR-29a-3p	Mix	1 nmol/L	1 h	[124]

续表

Method of detection	Sensor configuration	Technique	Capture element	Virus	Virus target	Sample solution	LOD	Time	Ref
Detect virus particles	Au film	SPR	Ab653, Ab956	FCV	FCV particles	Oyster matrix	-	15 min	[92]
	Ag-Au film	SPR	Anti-HA7 mAb	H7N9	H7N9 particles	PBS Nasal mucosa	144 copy/mL 402 copy/mL	10 min	[94]
ITO-Au nanopattern	Au film	LSPR	mAb 2G12	HIV	HIV-1 VLPs	DMEM	200 fg/mL	-	[20]
	Au film	SPR	-	H1N1	H1N1 particles	PBS	0.2 fg·mm ⁻²	-	[93]
Au film/AuNR	SPR	Anti-S protein Ab	SARS-CoV-2	SARS-CoV-2	SARS-CoV-2 particles	-	-	-	[97]
Au nanoparticle array/AuNPs	LSPR	Anti-S protein mAb	SARS-CoV-2	SARS-CoV-2	Pseudovirus particles	PBS	-	15 min	[98]
Au film	SPR	MIP	Bacteriophage	MSP2	MSP2	PBS	-	-	[99]
POF-Au film	SPR	MIP	SARS-CoV-2	SARS-CoV-2	SARS-CoV-2 particles	NaCl	-	10 min	[101]
Al ₂ O ₃ /Qdot-streptavidin	SPR	Anti-VLP mAb12A11	NV	NV	NV VLPs	PBS	0.01 ng/mL	-	[104]
AuNPs/CdSeTeS QDs	LSPR	Anti-HA Ab/ anti-NA Ab	H1N1	H1N1	H1N1 particles	Deionized water Serum	0.03 pg/mL 0.4 pg/mL	-	[106]
CdSeTeS QD-AuNP probe	LSPR	Anti-Nov Ab	NoV	NoV	NoVLPs	Deionized water	12.1×10 ⁻¹⁵ g/mL	1 min	[107]
QD-peptide-AuNP probe	LSPR	Anti-Ha Ab	H1N1	H1N1	H1N1 particles	Deionized water	17.02 fg/mL	-	[108]
QD-peptide-AuNP probe	LSPR	Anti-Nov Ab Anti-influenza Ab	NoV H1N1	NoV H1N1	NoVLPs H1N1 particles	Serum	124 fg/mL 14.6 fg/mL	-	[109]
	Au film	SPR	mAb	OMSV	OMSV particles	TE	1.36 ng/μL	30 min	[91]
Au film	SPR	Anti-MCMV Ab	MCMV	MCMV	MCMV virus	PBS	1×10 ⁻⁹	30 min	[90]
Au film	SPR	PAb/ mAb	PVY	PVY	PVY particles	-	0.31 μg/mL	-	[125]
AuNPs	LSPR	Anti-T7 Ab	Bacteriophage	Bacteriophage	T7	-	18 pmol/L	-	[126]
AuNPs	LSPR	IgG	DENV	DENV	DENV particles	PBS	-	5 min	[127]

Note: In "Sensor configuration" column, "/" means sandwich structure or layered structure, "-" indicates that a connection exists; SB, saliva buffer; PHEMAT film, poly(hydroxyethyl methacrylate-N-methacryloyl-L-tyrosine methyl ester) film; GBP, gold binding polypeptide; PA, protective antigen; BSA, bovine serum albumin; TE, tris-EDTA buffer solution; DEPC, diethyl pyrocarbonate; BSMV, barley stripe mosaic virus; EDTA, ethylene diamine tetraacetic acid; VLPs, virus-like particles; OMSV, oyster mushroom spherical virus; MCMV, maize chlorotic mottle virus; PVY, potato virus Y

参 考 文 献

- [1] Tscherné D M, García-Sastre A. Virulence determinants of pandemic influenza viruses [J]. *The Journal of Clinical Investigation*, 2011, 121(1): 6-13.
- [2] 张云辉, 赵雅琳, 闫晶晶, 等. 2021 年 8—9 月全球主要疫情回顾[J]. *传染病信息*, 2021, 34(5): 477-480.
Zhang Y H, Zhao Y L, Yan J J, et al. Review of the world's major epidemics from August to September in 2021 [J]. *Infectious Disease Information*, 2021, 34(5): 477-480.
- [3] Antiochia R. Developments in biosensors for CoV detection and future trends [J]. *Biosensors and Bioelectronics*, 2021, 173: 112777.
- [4] Cheng X H, Chen G, Rodriguez W R. Micro- and nanotechnology for viral detection [J]. *Analytical and Bioanalytical Chemistry*, 2009, 393(2): 487-501.
- [5] Carter L J, Garner L V, Smoot J W, et al. Assay techniques and test development for COVID-19 diagnosis [J]. *ACS Central Science*, 2020, 6(5): 591-605.
- [6] Ménard-Moyon C, Bianco A, Kalantar-Zadeh K. Two-dimensional material-based biosensors for virus detection [J]. *ACS Sensors*, 2020, 5(12): 3739-3769.
- [7] Ozer T, Geiss B J, Henry C S. Review-chemical and biological sensors for viral detection [J]. *Journal of the Electrochemical Society*, 2020, 167(3): 037523.
- [8] Burke D S, Nisalak A, Ussery M A. Antibody capture immunoassay detection of Japanese encephalitis virus immunoglobulin m and g antibodies in cerebrospinal fluid [J]. *Journal of Clinical Microbiology*, 1982, 16(6): 1034-1042.
- [9] Lu S M, Lin S, Zhang H R, et al. Methods of respiratory virus detection: advances towards point-of-care for early intervention [J]. *Micromachines*, 2021, 12(6): 697.
- [10] Vunsh R, Rosner A, Stein A. The use of the polymerase chain reaction (PCR) for the detection of bean yellow mosaic virus in gladiolus [J]. *Annals of Applied Biology*, 1990, 117(3): 561-569.
- [11] Boonham N, Kreuze J, Winter S, et al. Methods in virus diagnostics: from ELISA to next generation sequencing [J]. *Virus Research*, 2014, 186: 20-31.
- [12] Tam Y J, Zeenathul N A, Rezaei M A, et al. Wide dynamic range of surface-plasmon-resonance-based assay for hepatitis B surface antigen antibody optimal detection in comparison with ELISA [J]. *Biotechnology and Applied Biochemistry*, 2017, 64(5): 735-744.
- [13] Nguyen A H, Sim S J. Nanoplasmonic biosensor: detection and amplification of dual bio-signatures of circulating tumor DNA [J]. *Biosensors and Bioelectronics*, 2015, 67: 443-449.
- [14] Guo X W. Surface plasmon resonance based biosensor technique: a review [J]. *Journal of Biophotonics*, 2012, 5(7): 483-501.
- [15] Wang D P, Loo J F C, Chen J J, et al. Recent advances in surface plasmon resonance imaging sensors [J]. *Sensors*, 2019, 19(6): 1266.
- [16] Haes A J, Zou S L, Schatz G C, et al. A nanoscale optical biosensor: the long range distance dependence of the localized surface plasmon resonance of noble metal nanoparticles [J]. *The Journal of Physical Chemistry B*, 2004, 108(1): 109-116.
- [17] Liu X, Atwater M, Wang J H, et al. Extinction coefficient of gold nanoparticles with different sizes and different capping ligands [J]. *Colloids and Surfaces B: Biointerfaces*, 2007, 58(1): 3-7.
- [18] Nehl C L, Hafner J H. Shape-dependent plasmon resonances of gold nanoparticles [J]. *Journal of Materials Chemistry*, 2008, 18(21): 2415.
- [19] Sui M, Kunwar S, Pandey P, et al. Strongly confined localized surface plasmon resonance (LSPR) bands of Pt, AgPt, AgAuPt nanoparticles [J]. *Scientific Reports*, 2019, 9: 16582.
- [20] Lee J H, Kim B C, Oh B K, et al. Highly sensitive localized surface plasmon resonance immunosensor for label-free detection of HIV-1 [J]. *Nanomedicine: Nanotechnology, Biology and Medicine*, 2013, 9(7): 1018-1026.
- [21] Hassan M M, Sium F S, Islam F, et al. A review on plasmonic and metamaterial based biosensing platforms for virus detection [J]. *Sensing and Bio-Sensing Research*, 2021, 33: 100429.
- [22] Shrivastav A M, Cvelbar U, Abdulhalim I. A comprehensive review on plasmonic-based biosensors used in viral diagnostics [J]. *Communications Biology*, 2021, 4: 70.
- [23] Shi Y, Li Z, Liu P Y, et al. On-chip optical detection of viruses: a review [J]. *Advanced Photonics Research*, 2021, 2(4): 2000150.
- [24] Takemura K. Surface plasmon resonance (SPR)- and localized SPR (LSPR)-based virus sensing systems: optical vibration of nano- and micro-metallic materials for the development of next-generation virus detection technology [J]. *Biosensors*, 2021, 11(8): 250.
- [25] Slifka M K, Antia R, Whitmire J K, et al. Humoral immunity due to long-lived plasma cells [J]. *Immunity*, 1998, 8(3): 363-372.
- [26] Jeyanathan M, Afkhami S, Smaill F, et al. Immunological considerations for COVID-19 vaccine strategies [J]. *Nature Reviews Immunology*, 2020, 20(10): 615-632.
- [27] Bohn M K, Lippi G, Horvath A, et al. Molecular, serological, and biochemical diagnosis and monitoring of COVID-19: IFCC taskforce evaluation of the latest evidence [J]. *Clinical Chemistry and Laboratory Medicine*, 2020, 58(7): 1037-1052.
- [28] Younes N, Al-Sadeq D W, Al-Jighefee H, et al. Challenges in laboratory diagnosis of the novel coronavirus SARS-CoV-2 [J]. *Viruses*, 2020, 12(6): 582.
- [29] Hou H Y, Wang T, Zhang B, et al. Detection of IgM and IgG antibodies in patients with coronavirus disease 2019 [J]. *Clinical & Translational Immunology*, 2020, 9(5): e01136.
- [30] Zhang J, Zhang X M, Liu J H, et al. Serological detection of 2019-nCoV respond to the epidemic: a useful complement to nucleic acid testing [J]. *International Immunopharmacology*, 2020, 88: 106861.
- [31] Racine R, Winslow G M. IgM in microbial infections: taken for granted? [J]. *Immunology Letters*, 2009, 125(2): 79-85.
- [32] dos Santos G M C, Alves C R, Pinto M A, et al. Detection of antibodies against hepatitis A virus (HAV) by a surface plasmon resonance (SPR) biosensor: a new diagnosis tool based on the major HAV capsid protein VP₁ (SPR-HAVP₁) [J]. *Sensors*, 2021, 21(9): 3167.
- [33] 徐超, 王超群, 段志刚, 等. 基于原核表达鸭瘟病毒 gC 蛋白建立的表面等离子共振检测技术的研究 [J]. *中国兽医学*, 2020, 50(12): 1509-1514.
Xu C, Wang C Q, Duan Z G, et al. Identification of duck plague based on surface plasmon resonance with DPV gC prokaryotic expression protein [J]. *Chinese Veterinary Science*, 2020, 50(12): 1509-1514.
- [34] Basso C R, Malossi C D, Haisi A, et al. Fast and reliable detection of SARS-CoV-2 antibodies based on surface plasmon resonance [J]. *Analytical Methods: Advancing Methods and Applications*, 2021, 13(29): 3297-3306.
- [35] Jahanshahi P, Wei Q, Jie Z, et al. Kinetic analysis of IgM monoclonal antibodies for determination of dengue sample concentration using SPR technique [J]. *Bioengineered*, 2017, 8(3): 239-247.
- [36] Funari R, Chu K Y, Shen A Q. Detection of antibodies against SARS-CoV-2 spike protein by gold nanospikes in an opto-microfluidic chip [J]. *Biosensors and Bioelectronics*, 2020, 169: 112578.
- [37] Wang S H, Kuo C W, Lo S C, et al. Spectral image contrast-based flow digital nanoplasmon-metry for ultrasensitive antibody detection [J]. *Journal of Nanobiotechnology*, 2022, 20(1): 6.
- [38] Link S, El-Sayed M A. Simulation of the optical absorption spectra of gold nanorods as a function of their aspect ratio and

- the effect of the medium dielectric constant[J]. *The Journal of Physical Chemistry B*, 2005, 109(20): 10531-10532.
- [39] Lee K S, El-Sayed M A. Gold and silver nanoparticles in sensing and imaging: sensitivity of plasmon response to size, shape, and metal composition[J]. *The Journal of Physical Chemistry B*, 2006, 110(39): 19220-19225.
- [40] Jain P K, Eustis S, El-Sayed M A. Plasmon coupling in nanorod assemblies: optical absorption, discrete dipole approximation simulation, and exciton-coupling model [J]. *The Journal of Physical Chemistry B*, 2006, 110(37): 18243-18253.
- [41] Versiani A F, Martins E M N, Andrade L M, et al. Nanosensors based on LSPR are able to serologically differentiate dengue from Zika infections[J]. *Scientific Reports*, 2020, 10: 11302.
- [42] Jiang Q S, Chandar Y J, Cao S S, et al. Rapid, point-of-care, paper-based plasmonic biosensor for zika virus diagnosis [J]. *Advanced Biosystems*, 2017, 1(9): e1700096.
- [43] Huang H W, Tang C R, Zeng Y L, et al. Label-free optical biosensor based on localized surface plasmon resonance of immobilized gold nanorods [J]. *Colloids and Surfaces B: Biointerfaces*, 2009, 71(1): 96-101.
- [44] 金子铮, 金方方, 刘新, 等. HBsAg 与抗-HBs 共阳性血清学模式的产生机制及临床意义[J]. *检验医学与临床*, 2019, 16(4): 566-571.
Jin Z Z, Jin F F, Liu X, et al. Mechanism and clinical significance of co-positive serological pattern of HBsAg and anti-HBs[J]. *Laboratory Medicine and Clinic*, 2019, 16(4): 566-571.
- [45] Leary T P, Gutierrez R A, Muerhoff A S, et al. A chemiluminescent, magnetic particle-based immunoassay for the detection of hepatitis C virus core antigen in human serum or plasma[J]. *Journal of Medical Virology*, 2006, 78(11): 1436-1440.
- [46] Laperche S, Nübling C M, Stramer S L, et al. Sensitivity of hepatitis C virus core antigen and antibody combination assays in a global panel of window period samples[J]. *Transfusion*, 2015, 55(10): 2489-2498.
- [47] Ly T D, Ebel A, Faucher V, et al. Could the new HIV combined p24 antigen and antibody assays replace p24 antigen specific assays? [J]. *Journal of Virological Methods*, 2007, 143(1): 86-94.
- [48] Sarcina L, Mangiatordi G F, Torricelli F, et al. Surface plasmon resonance assay for label-free and selective detection of HIV-1 p24 protein[J]. *Biosensors*, 2021, 11(6): 180.
- [49] Sharma P K, Kumar J S, Singh V V, et al. Surface plasmon resonance sensing of Ebola virus: a biological threat [J]. *Analytical and Bioanalytical Chemistry*, 2020, 412(17): 4101-4112.
- [50] 陆彩燕, 李勇萍, 袁玉峰, 等. 二维 $Ti_3C_2T_x$ MXene 纳米薄层用于超灵敏等离子体生化传感的研究[J]. *激光与光电子学进展*, 2020, 57(9): 091601.
Lu C Y, Li Y P, Yuan Y F, et al. Ultrasensitive biochemical detection by employing two-dimensional $Ti_3C_2T_x$ MXene nanosheets[J]. *Laser & Optoelectronics Progress*, 2020, 57(9): 091601.
- [51] 彭芳, 张良, 何建安. 石墨烯增敏的 SPR 技术应用于 HIV1 p24 抗原的检测[J]. *生物化工*, 2021, 7(3): 4-8.
Peng F, Zhang L, He J A. Graphene assisted detection of HIV₁ p24 antigen by surface plasmon resonance technique[J]. *Biological Chemical Engineering*, 2021, 7(3): 4-8.
- [52] Omar N A S, Fen Y W, Abdullah J, et al. Development of an optical sensor based on surface plasmon resonance phenomenon for diagnosis of dengue virus E-protein[J]. *Sensing and Bio-Sensing Research*, 2018, 20: 16-21.
- [53] Omar N A S, Fen Y W, Abdullah J, et al. Sensitive detection of dengue virus type 2 E-proteins signals using self-assembled monolayers/reduced graphene oxide-PAMAM dendrimer thin film-SPR optical sensor[J]. *Scientific Reports*, 2020, 10: 2374.
- [54] Omar N A S, Fen Y W, Abdullah J, et al. Quantitative and selective surface plasmon resonance response based on a reduced graphene oxide-polyamidoamine nanocomposite for detection of dengue virus E-proteins[J]. *Nanomaterials*, 2020, 10(3): 569.
- [55] Qatamin A H, Ghithan J H, Moreno M, et al. Detection of influenza virus by electrochemical surface plasmon resonance under potential modulation[J]. *Applied Optics*, 2019, 58(11): 2839-2844.
- [56] Bruce-Staskal P J, Woods R M, Borisov O V, et al. Hemagglutinin from multiple divergent influenza A and B viruses bind to a distinct branched, sialylated poly-LacNAc glycan by surface plasmon resonance[J]. *Vaccine*, 2020, 38(43): 6757-6765.
- [57] 洪小刚, 徐文东, 赵成强, 等. 表面等离子体共振膜系结构优化设计[J]. *光学学报*, 2010, 30(7): 2164-2169.
Hong X G, Xu W D, Zhao C Q, et al. Optimal design of surface plasmon resonance films structure [J]. *Acta Optica Sinica*, 2010, 30(7): 2164-2169.
- [58] Murat N F, Mukhtar W M, Rashid A R A, et al. Optimization of gold thin films thicknesses in enhancing SPR response[C]// 2016 IEEE International Conference on Semiconductor Electronics, August 17-19, 2016, Kuala Lumpur, Malaysia. New York: IEEE Press, 2016: 244-247.
- [59] Kim J, Oh S Y, Shukla S, et al. Heteroassembled gold nanoparticles with sandwich-immunoassay LSPR chip format for rapid and sensitive detection of hepatitis B virus surface antigen (HBsAg) [J]. *Biosensors and Bioelectronics*, 2018, 107: 118-122.
- [60] Heo N S, Oh S Y, Ryu M Y, et al. Affinity peptide-guided plasmonic biosensor for detection of noroviral protein and human norovirus[J]. *Biotechnology and Bioprocess Engineering*, 2019, 24(2): 318-325.
- [61] Lewis T, Giroux E, Jovic M, et al. Localized surface plasmon resonance aptasensor for selective detection of SARS-CoV-2 S1 protein[J]. *The Analyst*, 2021, 146(23): 7207-7217.
- [62] Lee T, Kim G H, Kim S M, et al. Label-free localized surface plasmon resonance biosensor composed of multi-functional DNA 3 way junction on hollow Au spike-like nanoparticles (HAuSN) for avian influenza virus detection[J]. *Colloids and Surfaces B: Biointerfaces*, 2019, 182: 110341.
- [63] Diltemiz S E, Ersöz A, Hür D, et al. 4-Aminophenyl boronic acid modified gold platforms for influenza diagnosis [J]. *Materials Science and Engineering: C*, 2013, 33(2): 824-830.
- [64] Zang F H, Su Z J, Zhou L C, et al. Ultrasensitive Ebola virus antigen sensing via 3D nanoantenna arrays [J]. *Advanced Materials*, 2019, 31(30): e1902331.
- [65] Takemura K, Adegoke O, Suzuki T, et al. A localized surface plasmon resonance-amplified immunofluorescence biosensor for ultrasensitive and rapid detection of nonstructural protein 1 of Zika virus[J]. *PLoS One*, 2019, 14(1): e0211517.
- [66] Bailey R E, Smith A M, Nie S M. Quantum dots in biology and medicine [J]. *Physica E: Low-Dimensional Systems and Nanostructures*, 2004, 25(1): 1-12.
- [67] Mateu M G. Structure and physics of viruses[M]. Dordrecht: Springer, 2013.
- [68] Kim S A, Kim S J, Lee S H, et al. Detection of avian influenza-DNA hybridization using wavelength-scanning surface plasmon resonance biosensor[J]. *Journal of the Optical Society of Korea*, 2009, 13(3): 392-397.
- [69] Das S, Agarwal D K, Mandal B, et al. Detection of the chilli leaf curl virus using an attenuated total reflection-mediated localized surface-plasmon-resonance-based optical platform [J]. *ACS Omega*, 2021, 6(27): 17413-17423.
- [70] Moitra P, Alafeef M, Dighe K, et al. Selective naked-eye detection of SARS-CoV-2 mediated by N gene targeted antisense oligonucleotide capped plasmonic nanoparticles [J]. *ACS Nano*, 2020, 14(6): 7617-7627.
- [71] He P, Qiao W P, Liu L J, et al. A highly sensitive surface

- plasmon resonance sensor for the detection of DNA and cancer cells by a target-triggered multiple signal amplification strategy [J]. *Chemical Communications*, 2014, 50(73): 10718-10721.
- [72] He P, Liu L J, Qiao W P, et al. Ultrasensitive detection of thrombin using surface plasmon resonance and quartz crystal microbalance sensors by aptamer-based rolling circle amplification and nanoparticle signal enhancement [J]. *Chemical Communications*, 2014, 50(12): 1481-1484.
- [73] Chuang T L, Wei S C, Lee S Y, et al. A polycarbonate based surface plasmon resonance sensing cartridge for high sensitivity HBV loop-mediated isothermal amplification [J]. *Biosensors and Bioelectronics*, 2012, 32(1): 89-95.
- [74] Lugongolo M Y, Manoto S, Maphanga C, et al. Label-free detection of mutations in the HIV genome using a surface plasmon resonance biosensor [J]. *Proceedings of SPIE*, 2021, 11661: 116610M.
- [75] 廖婧, 许长俊, 孙春意, 等. hTERC 基因检测与 HC2、SPR 技术检测 HPV 在宫颈病变中的诊断价值 [J]. *昆明医科大学学报*, 2020, 41(9): 17-20.
- Liao J, Xu C J, Sun C Y, et al. The diagnostic value of hTERC gene detection and HC2 and SPR technology in detecting HPV in cervical lesions [J]. *Journal of Kunming Medical University*, 2020, 41(9): 17-20.
- [76] Miao Y B, Ren H X, Gan N, et al. A triple-amplification SPR electrochemiluminescence assay for chloramphenicol based on polymer enzyme-linked nanotracers and exonuclease-assisted target recycling [J]. *Biosensors and Bioelectronics*, 2016, 86: 477-483.
- [77] Diao W, Tang M, Ding S J, et al. Highly sensitive surface plasmon resonance biosensor for the detection of HIV-related DNA based on dynamic and structural DNA nanodevices [J]. *Biosensors and Bioelectronics*, 2018, 100: 228-234.
- [78] Zhou C, Zou H M, Sun C J, et al. Signal amplification strategies for DNA-based surface plasmon resonance biosensors [J]. *Biosensors and Bioelectronics*, 2018, 117: 678-689.
- [79] Shi D C, Huang J F, Chuai Z R, et al. Isothermal and rapid detection of pathogenic microorganisms using a nano-rolling circle amplification-surface plasmon resonance biosensor [J]. *Biosensors and Bioelectronics*, 2014, 62: 280-287.
- [80] Li Y H, Yan Y R, Lei Y N, et al. Surface plasmon resonance biosensor for label-free and highly sensitive detection of point mutation using polymerization extension reaction [J]. *Colloids and Surfaces B: Biointerfaces*, 2014, 120: 15-20.
- [81] Knez K, Spasic D, Delpont F, et al. Real-time ligation chain reaction for DNA quantification and identification on the FO-SPR [J]. *Biosensors and Bioelectronics*, 2015, 67: 394-399.
- [82] Lin Z N, Chen S J, Lin C Y. Sensitivity improvement of a surface plasmon resonance sensor based on two-dimensional materials hybrid structure in visible region: a theoretical study [J]. *Sensors*, 2020, 20(9): 2445.
- [83] Akib T B A, Mou S F, Rahman M M, et al. Design and numerical analysis of a graphene-coated SPR biosensor for rapid detection of the novel coronavirus [J]. *Sensors*, 2021, 21(10): 3491.
- [84] Liu L X, Ye K, Jia Z Y, et al. High-sensitivity and versatile plasmonic biosensor based on grain boundaries in polycrystalline 1L WS₂ films [J]. *Biosensors and Bioelectronics*, 2021, 194: 113596.
- [85] Chowdhury A D, Takemura K, Khorish I M, et al. The detection and identification of dengue virus serotypes with quantum dot and AuNP regulated localized surface plasmon resonance [J]. *Nanoscale Advances*, 2020, 2(2): 699-709.
- [86] Adegoke O, Morita M, Kato T, et al. Localized surface plasmon resonance-mediated fluorescence signals in plasmonic nanoparticle-quantum dot hybrids for ultrasensitive Zika virus RNA detection via hairpin hybridization assays [J]. *Biosensors and Bioelectronics*, 2017, 94: 513-522.
- [87] Qiu G Y, Gai Z B, Tao Y L, et al. Dual-functional plasmonic photothermal biosensors for highly accurate severe acute respiratory syndrome coronavirus 2 detection [J]. *ACS Nano*, 2020, 14(5): 5268-5277.
- [88] Qiu G Y, Gai Z B, Saleh L, et al. Thermoplasmonic-assisted cyclic cleavage amplification for self-validating plasmonic detection of SARS-CoV-2 [J]. *ACS Nano*, 2021, 15(4): 7536-7546.
- [89] Su L C, Chang C M, Tseng Y L, et al. Rapid and highly sensitive method for influenza A (H1N1) virus detection [J]. *Analytical Chemistry*, 2012, 84(9): 3914-3920.
- [90] Zeng C, Huang X, Xu J M, et al. Rapid and sensitive detection of maize chlorotic mottle virus using surface plasmon resonance-based biosensor [J]. *Analytical Biochemistry*, 2013, 440(1): 18-22.
- [91] Kim S W, Kim M G, Kim J, et al. Detection of the mycovirus OMSV in the edible mushroom, *pleurotus ostreatus*, using an SPR biosensor chip [J]. *Journal of Virological Methods*, 2008, 148(1/2): 120-124.
- [92] Yakes B J, Papafragkou E, Conrad S M, et al. Surface plasmon resonance biosensor for detection of feline calicivirus, a surrogate for norovirus [J]. *International Journal of Food Microbiology*, 2013, 162(2): 152-158.
- [93] Wang S P, Shan X N, Patel U, et al. Label-free imaging, detection, and mass measurement of single viruses by surface plasmon resonance [J]. *Proceedings of the National Academy of Sciences of the United States of America*, 2010, 107(37): 16028-16032.
- [94] Chang Y F, Wang W H, Hong Y W, et al. Simple strategy for rapid and sensitive detection of avian influenza A H₇N₉ virus based on intensity-modulated SPR biosensor and new generated antibody [J]. *Analytical Chemistry*, 2018, 90(3): 1861-1869.
- [95] Bai Y F, Feng F, Zhao L, et al. Aptamer/thrombin/antibody-AuNPs sandwich enhanced surface plasmon resonance sensor for the detection of subnanomolar thrombin [J]. *Biosensors and Bioelectronics*, 2013, 47: 265-270.
- [96] Szunerits S, Spadavecchia J, Boukherroub R. Surface plasmon resonance: signal amplification using colloidal gold nanoparticles for enhanced sensitivity [J]. *Reviews in Analytical Chemistry*, 2014, 33(3): 153-164.
- [97] Das C M, Guo Y, Yang G, et al. Gold nanorod assisted enhanced plasmonic detection scheme of COVID-19 SARS-CoV-2 spike protein [J]. *Advanced Theory and Simulations*, 2020, 3(11): 2000185.
- [98] Huang L P, Ding L F, Zhou J, et al. One-step rapid quantification of SARS-CoV-2 virus particles via low-cost nanoplasmonic sensors in generic microplate reader and point-of-care device [J]. *Biosensors and Bioelectronics*, 2021, 171: 112685.
- [99] Altintas Z, Gittens M, Guerreiro A, et al. Detection of waterborne viruses using high affinity molecularly imprinted polymers [J]. *Analytical Chemistry*, 2015, 87(13): 6801-6807.
- [100] Malik A A, Nantasenamat C, Piacham T. Molecularly imprinted polymer for human viral pathogen detection [J]. *Materials Science and Engineering: C*, 2017, 77: 1341-1348.
- [101] Cennamo N, D'Agostino G, Perri C, et al. Proof of concept for a quick and highly sensitive on-site detection of SARS-CoV-2 by plasmonic optical fibers and molecularly imprinted polymers [J]. *Sensors*, 2021, 21(5): 1681.
- [102] Jing J Y, Liu K, Jiang J F, et al. Performance improvement approaches for optical fiber SPR sensors and their sensing applications [J]. *Photonics Research*, 2022, 10(1): 126-147.
- [103] 马金英, 刘铁根, 江俊峰, 等. 光纤表面等离子体共振传感灵敏度提高研究进展 [J]. *中国激光*, 2021, 48(19): 1906002.
- Ma J Y, Liu T G, Jiang J F, et al. Progress in sensitivity enhancement for optical fibre surface plasmon resonance sensing [J]. *Chinese Journal of Lasers*, 2021, 48(19): 1906002.

- [104] Ashiba H, Sugiyama Y, Wang X M, et al. Detection of norovirus virus-like particles using a surface plasmon resonance-assisted fluoroimmunosensor optimized for quantum dot fluorescent labels[J]. *Biosensors and Bioelectronics*, 2017, 93: 260-266.
- [105] Chang Y F, Wang S F, Huang J C, et al. Detection of swine-origin influenza A (H1N1) viruses using a localized surface plasmon coupled fluorescence fiber-optic biosensor [J]. *Biosensors and Bioelectronics*, 2010, 26(3): 1068-1073.
- [106] Takemura K, Adegoko O, Takahashi N, et al. Versatility of a localized surface plasmon resonance-based gold nanoparticle-alloyed quantum dot nanobiosensor for immunofluorescence detection of viruses[J]. *Biosensors and Bioelectronics*, 2017, 89: 998-1005.
- [107] Nasrin F, Chowdhury A D, Takemura K, et al. Single-step detection of norovirus tuning localized surface plasmon resonance-induced optical signal between gold nanoparticles and quantum dots [J]. *Biosensors and Bioelectronics*, 2018, 122: 16-24.
- [108] Nasrin F, Chowdhury A D, Takemura K, et al. Fluorometric virus detection platform using quantum dots-gold nanocomposites optimizing the linker length variation [J]. *Analytica Chimica Acta*, 2020, 1109: 148-157.
- [109] Chowdhury A D, Nasrin F, Gangopadhyay R, et al. Controlling distance, size and concentration of nanoconjugates for optimized LSPR based biosensors [J]. *Biosensors and Bioelectronics*, 2020, 170: 112657.
- [110] Riedel T, Rodriguez-Emmenegger C, de los Santos Pereira A, et al. Diagnosis of Epstein-Barr virus infection in clinical serum samples by an SPR biosensor assay [J]. *Biosensors and Bioelectronics*, 2014, 55: 278-284.
- [111] Riedel T, Surman F, Hageneder S, et al. Hepatitis B plasmonic biosensor for the analysis of clinical serum samples [J]. *Biosensors and Bioelectronics*, 2016, 85: 272-279.
- [112] Yoo H, Shin J, Sim J, et al. Reusable surface plasmon resonance biosensor chip for the detection of H1N1 influenza virus[J]. *Biosensors and Bioelectronics*, 2020, 168: 112561.
- [113] Goode J A, Rushworth J V H, Millner P A. Biosensor regeneration: a review of common techniques and outcomes [J]. *Langmuir: the ACS Journal of Surfaces and Colloids*, 2015, 31(23): 6267-6276.
- [114] Uzun L, Say R, Ünal S, et al. Production of surface plasmon resonance based assay kit for hepatitis diagnosis[J]. *Biosensors and Bioelectronics*, 2009, 24(9): 2878-2884.
- [115] Park T J, Lee S J, Kim D K, et al. Development of label-free optical diagnosis for sensitive detection of influenza virus with genetically engineered fusion protein[J]. *Talanta*, 2012, 89: 246-252.
- [116] Jahanshahi P, Zalnezhad E, Sekaran S D, et al. Rapid immunoglobulin M-based dengue diagnostic test using surface plasmon resonance biosensor[J]. *Scientific Reports*, 2014, 4: 3851.
- [117] Im H, Sutherland J N, Maynard J A, et al. Nanohole-based surface plasmon resonance instruments with improved spectral resolution quantify a broad range of antibody-ligand binding kinetics[J]. *Analytical Chemistry*, 2012, 84(4): 1941-1947.
- [118] Kumbhat S, Sharma K, Gehlot R, et al. Surface plasmon resonance based immunosensor for serological diagnosis of dengue virus infection [J]. *Journal of Pharmaceutical and Biomedical Analysis*, 2010, 52(2): 255-259.
- [119] Wong C L, Chua M, Mittman H, et al. A phase-intensity surface plasmon resonance biosensor for avian influenza A (H5N1) detection[J]. *Sensors*, 2017, 17(10): 2363.
- [120] Nilsson C E, Abbas S, Bennemo M, et al. A novel assay for influenza virus quantification using surface plasmon resonance [J]. *Vaccine*, 2010, 28(3): 759-766.
- [121] Wang X H, Li Y, Wang H F, et al. Gold nanorod-based localized surface plasmon resonance biosensor for sensitive detection of hepatitis B virus in buffer, blood serum and plasma [J]. *Biosensors and Bioelectronics*, 2010, 26(2): 404-410.
- [122] Vidic J, Chevalier C, Le Goffic R, et al. Surface plasmon resonance immunosensor for detection of PB1-F2 influenza A virus protein in infected biological samples [J]. *Journal of Analytical & Bioanalytical Techniques*, 2013, S7: 6.
- [123] Florschütz K, Schröter A, Schmieder S, et al. 'Phytochip': on-chip detection of phytopathogenic RNA viruses by a new surface plasmon resonance platform[J]. *Journal of Virological Methods*, 2013, 189(1): 80-86.
- [124] Loo J F C, Wang S S, Peng F, et al. A non-PCR SPR platform using RNase H to detect microRNA 29a-3p from throat swabs of human subjects with influenza A virus H1N1 infection[J]. *The Analyst*, 2015, 140(13): 4566-4575.
- [125] Gutiérrez-Aguirre I, Hodnik V, Glais L, et al. Surface plasmon resonance for monitoring the interaction of Potato virus Y with monoclonal antibodies [J]. *Analytical Biochemistry*, 2014, 447: 74-81.
- [126] Lesniewski A, Los M, Jonsson-Niedziółka M, et al. Antibody modified gold nanoparticles for fast and selective, colorimetric T7 bacteriophage detection[J]. *Bioconjugate Chemistry*, 2014, 25(4): 644-648.
- [127] Basso C R, Tozato C C, Crulhas B P, et al. An easy way to detect dengue virus using nanoparticle-antibody conjugates[J]. *Virology*, 2018, 513: 85-90.

Research Progress of Surface Plasmon Resonance and Local Surface Plasmon Resonance in Virus Detection

Xu Houxiang, Xu Bin^{***}, Xiong Jichuan^{**}, Liu Xuefeng^{*}

School of Electronic and Optical Engineering, Nanjing University of Science and Technology, Nanjing 210094, Jiangsu, China

Abstract

Significance In 2009, influenza A (H1N1) broke out in Mexico and the United States, influencing 214 countries and killing at least 14000 people. The novel coronavirus epidemic which broke out in 2020 has still been raging all over the world for two years as the results of the huge difficulty in the rapid and real-time epidemic prevention detection and the other reasons. In addition, the spread of other viruses including dengue virus (DENV) and human immunodeficiency virus (HIV) is also threatening human health significantly. Virus detection is the key to curb the spread of the viruses.

At present, enzyme-linked immunosorbent assay (ELISA) and polymerase chain reaction (PCR), as the gold standard

in the field of virus detection, can be used to detect and trace virus samples with a high sensitivity. But these samples need to be collected to the laboratory, and the viruses must be isolated and determined using the sophisticated lab equipment operated by professionals in order to get accurate results. Surface plasmon resonance (SPR) and local surface plasmon resonance (LSPR) biosensors may be an effective alternative, as their structures are simple and easy to be miniaturized. Especially, the LSPR-based device only needs a light source and some sensing elements. Once the sensing elements successfully capture the virus, the detection process will be quickly, sensitively, and selectively finished. These characteristics of the SPR and LSPR techniques show their great application potential in the field of virus detection, especially for the point-of-care testing with limited conditions.

With the rapid development of SPR and LSPR-based virus detection researches, researchers have reviewed the progress of materials and structures of sensors, methods for plasmonic virus detection, and their characteristics of signal amplification, and so on. According to the four general virus detection methods and starting from the four kinds of target analytes captured by the sensor, this paper systematically outlines the latest researches of the SPR and LSPR techniques for detecting viruses, which are of great significance for their clinical application (Fig. 1).

Progress First, according to the four methods for virus detection, the application progress of SPR and LSPR in the fields of antibody, antigen, nucleic acid, and virus particle detection is reviewed successively. For the SPR or LSPR sensors based on the binding principle of specific antigen-antibodies, the detection limit is further optimized by modifying the appropriate antigens or antibodies. More stable and inexpensive aptamers and molecularly imprinted polymers are expected to replace antibodies as sensor recognition elements to detect virus antigens or particles. Because the number of virus genomes in clinical samples is usually very small, the detection of nucleic acid by SPR or LSPR alone is limited. However, the detection of virus samples with the concentration at the femto scale can be realized by combining SPR or LSPR with DNA amplification and fluorescent substances. Second, the problems of biological medium contamination and repeatability encountered by biosensors as well as their solutions are introduced (Fig. 13). As for the contamination of biological media, self-assembled monolayers (SAM) can be synthesized on the surface of sensor elements to alleviate this problem. Riedel *et al.* further reduced or even completely inhibited the biological contamination of plasma and serum by synthesizing polymer brushes. In order to ensure the repeatability of sensing elements, Yoo *et al.* used magnetic beads replaced under the control of magnetic field as the sensing element, allowing that the sensor chip could still work stably after many repeated measurements. Third, the configurations and parameters of the SPR and LSPR sensors for virus detection in the past 15 years are listed (Table 1), and the advantages of the SPR and LSPR techniques are described. Finally, the optimization strategies of the SPR and LSPR techniques and the present existing problems are summarized. Moreover, the application prospect is also forecasted.

Conclusion and Prospect According to the current research progress, the optimization strategy of the SPR sensor mainly focuses on film material sensitization and metal particle coupling sensitization. The former includes the application of 2D materials and molecular imprinting through the construction of surface films to enhance practicality and applicability. In contrast, the latter uses nanoparticles to form sandwich structures. The LSPR sensing strategies are concentrated on the design and optimization of nanoparticles or nanostructures, which are often combined with fluorescent substances such as quantum dots (QDs) to form sensing probes for virus detection by the light absorption peak shift or the fluorescence intensity change. The LSPR biosensors are normally easier to be miniaturized than the SPR counterparts. In a word, the SPR and LSPR sensors show great application prospects in the field of virus detection. Predictably, owing to the diversity of the SPR and LSPR virus sensor modifiers, it may be possible to detect specific viruses for multiple target analytes at the same time through the integration of sensor recognition elements, which enables the multi-dimensional evaluation of virus infection in a short time to avoid false negative and false positive cases.

Key words biotechnology; surface plasmon; surface plasmon resonance; local surface plasmon resonance; virus detection; biosensor